

Metal-Organic Frameworks for Sustainable Catalysis and Artificial Photosynthesis

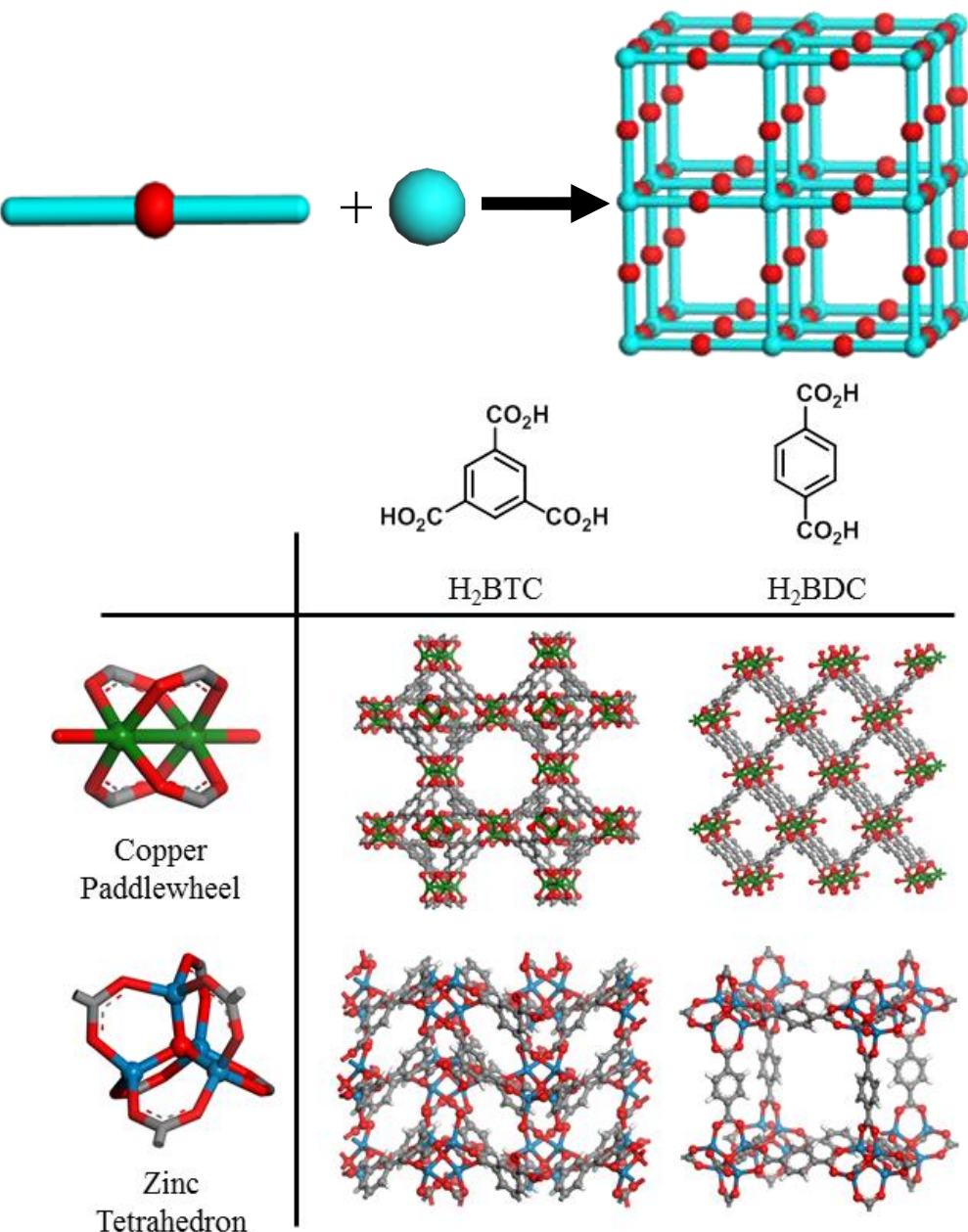
Wenbin Lin

Department of Chemistry
The University of Chicago
Chicago, IL 60637

wenbinlin@uchicago.edu
<http://linlab.uchicago.edu>

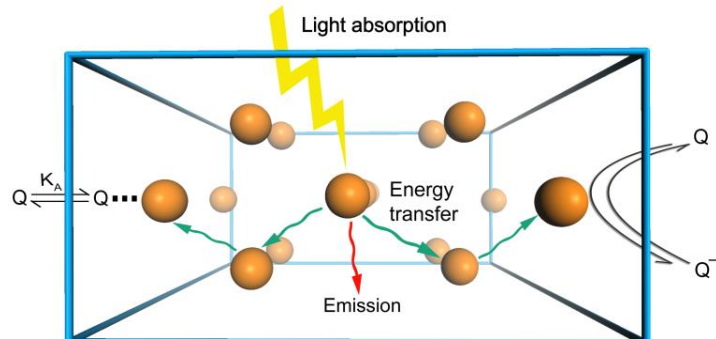
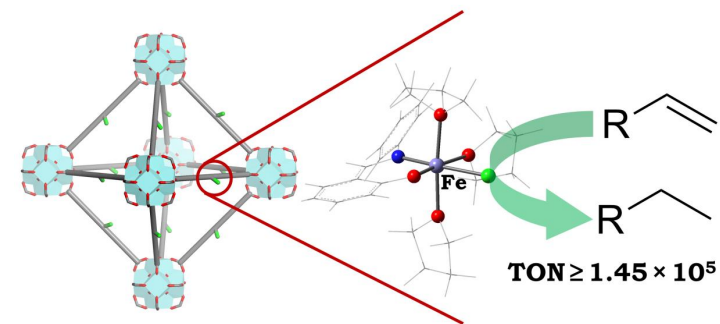
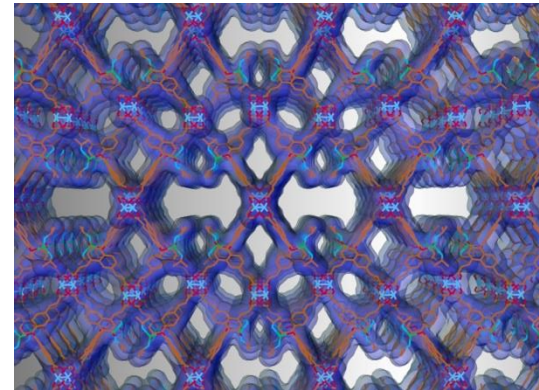
Coordination Polymers/Coordination Networks/Metal-Organic Frameworks

- Crystallinity
 - Highly ordered periodic structure
 - Allows structural determination, investigation of structure-activity relationships
- Reticular synthesis
 - Rational “design” using molecular building units
 - Shape of ligand and metal connecting point determine connectivity of final material
- Ease of Imparting Functionality
 - Mild synthetic preparation
 - Bridging ligands can contain a secondary functional group, which can be modified or used directly upon MOF preparation

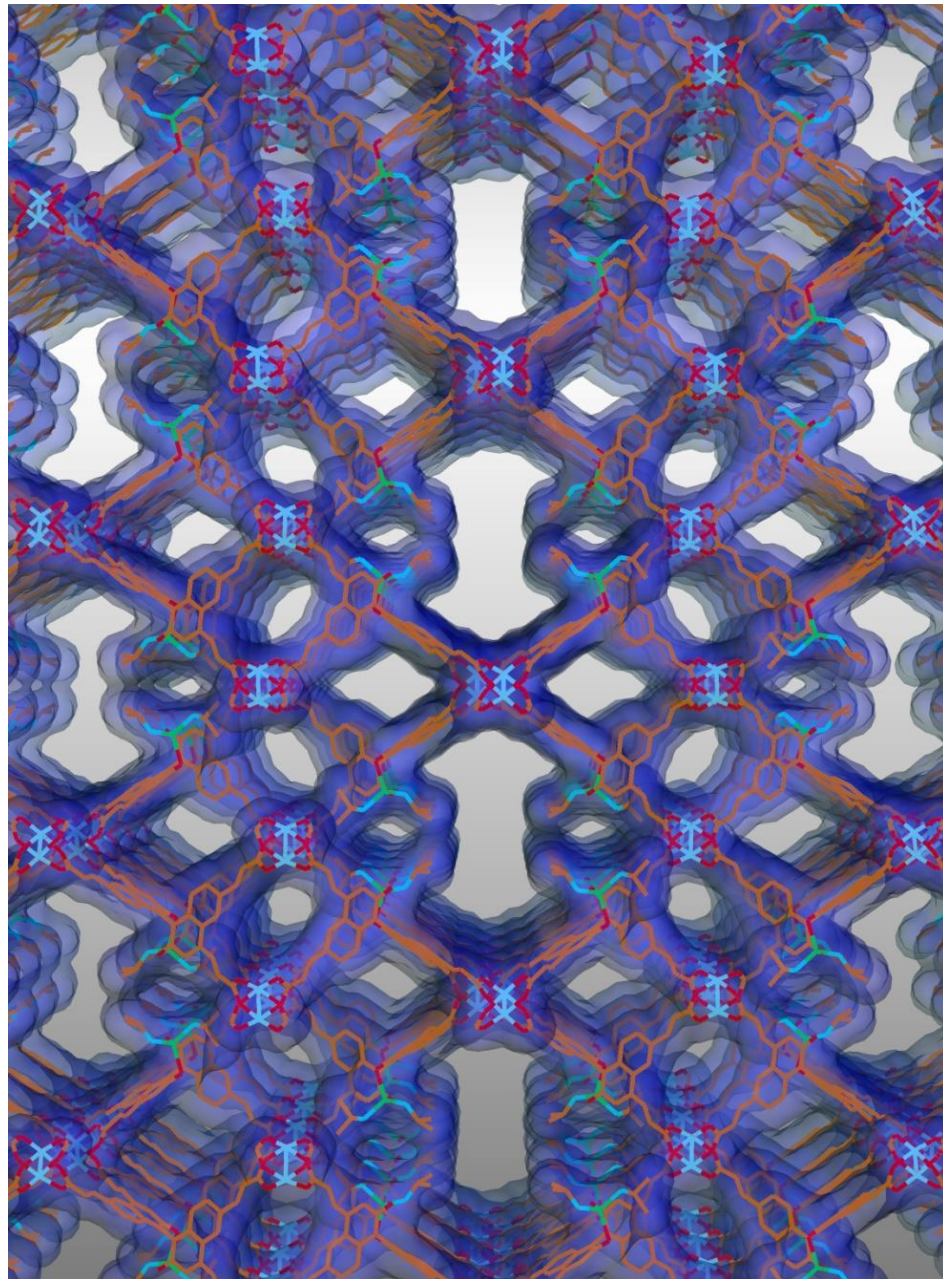


Talk Outline

- ◆ Chiral MOFs as Single-Site Solid Asymmetric Catalysts
- ◆ MOFs as A New Platform for Discovering Base-Metal Catalysts
- ◆ MOFs for Artificial Photosynthesis and Photocatalysis



Metal-Organic Frameworks as Single-Site Solid Asymmetric Catalysts



Chiral channels of several nanometers in dimensions would be needed to allow the diffusion of substrates and products.

Identical catalyst sites in the solid material

Size- and enantio-selectivity

Recyclability and re-usability

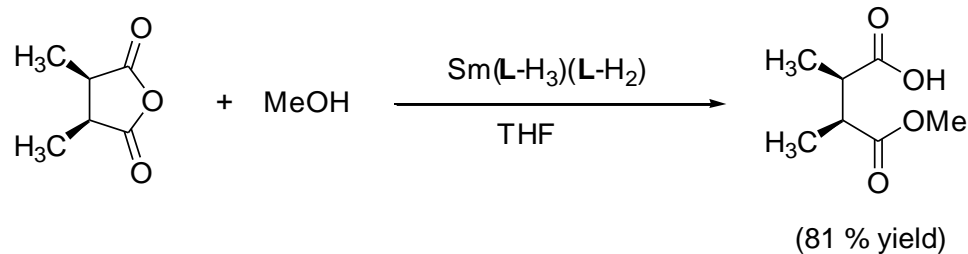
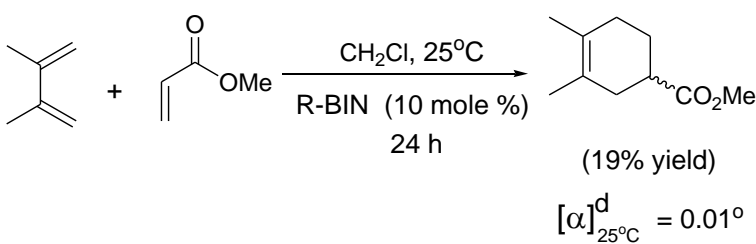
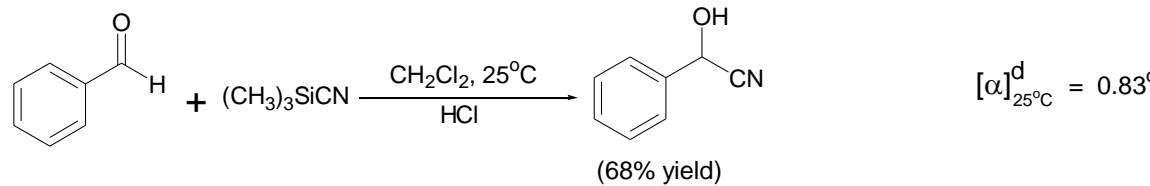
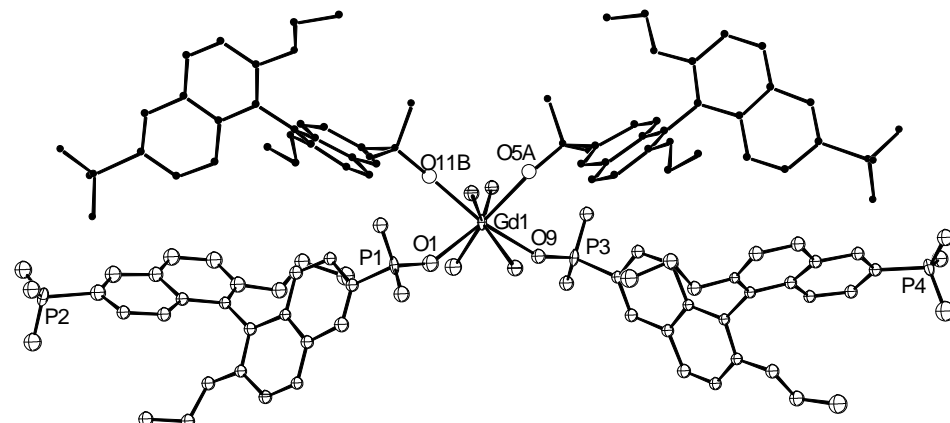
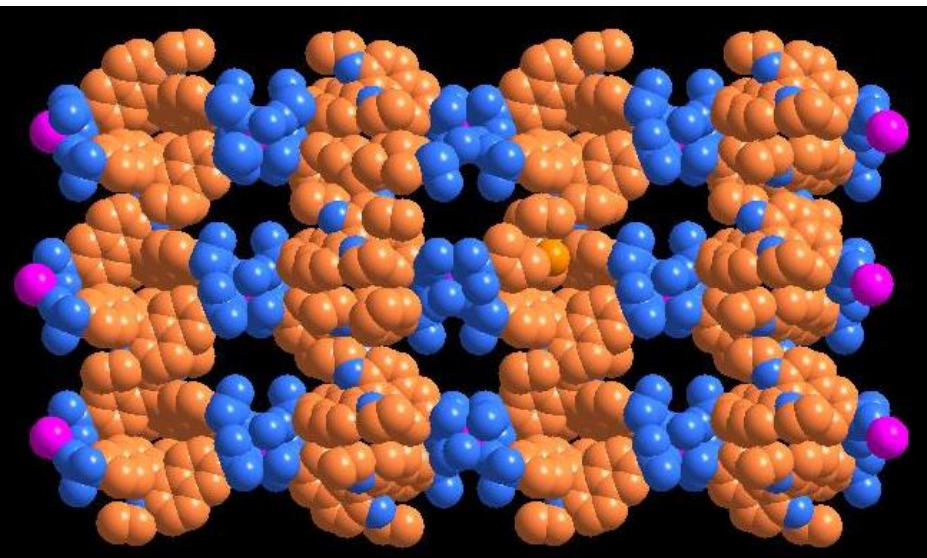
Synthetic tunability

Enhanced catalytic activity

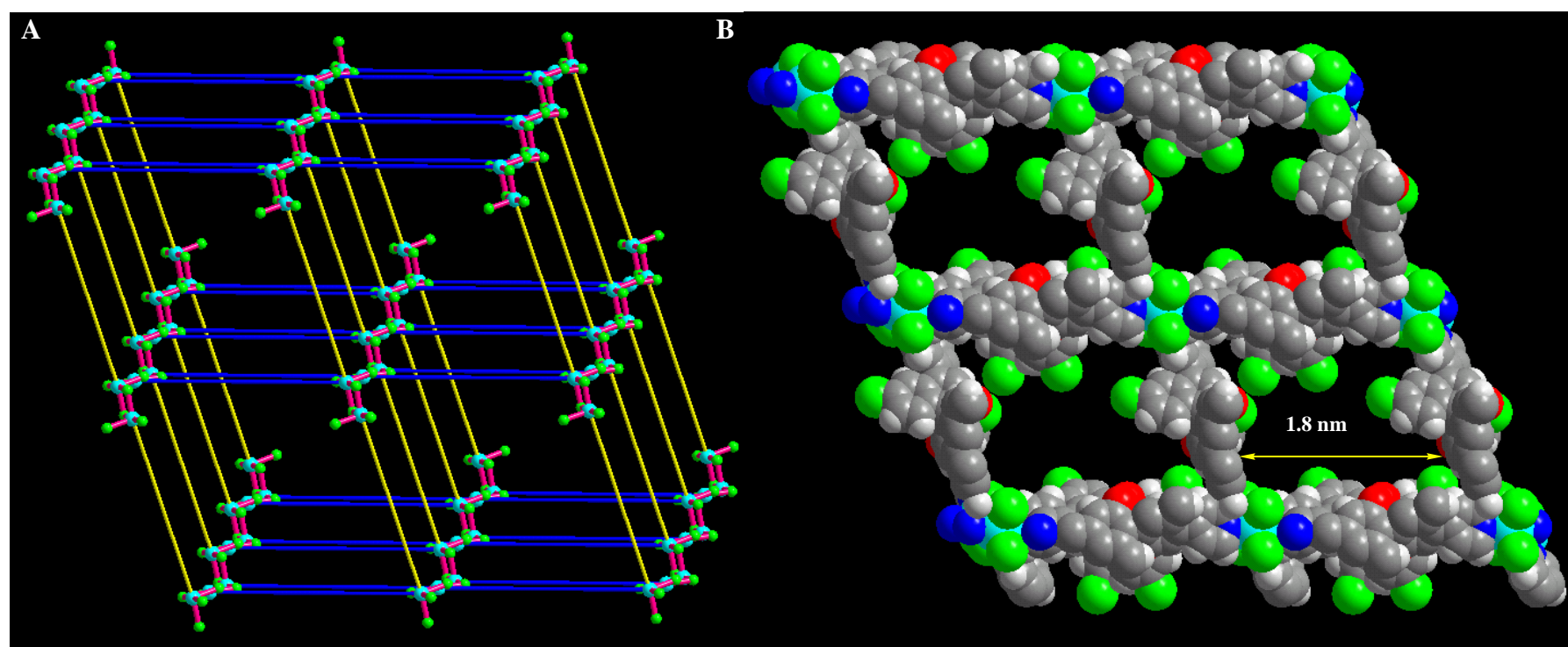
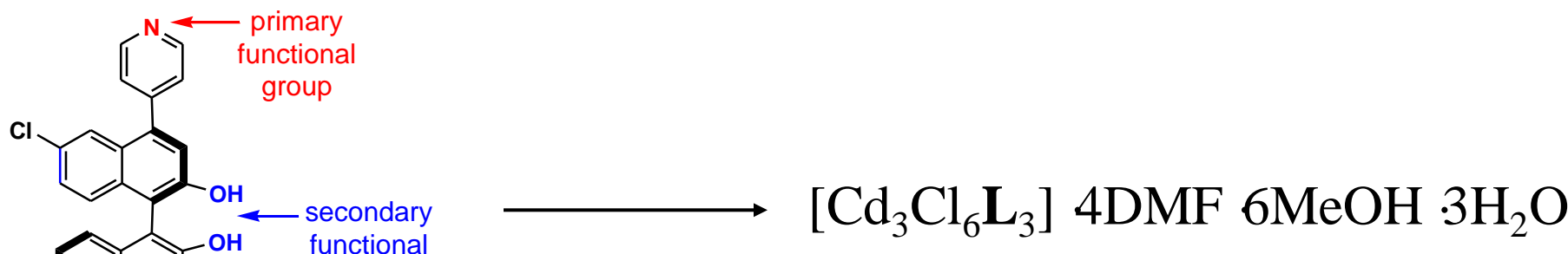
Unique reactivity

Practical utility?

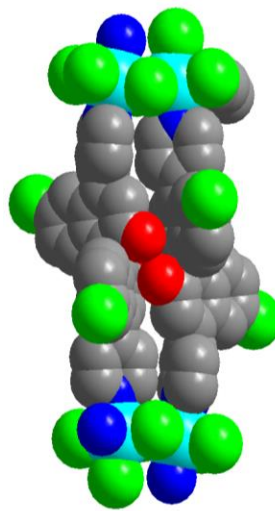
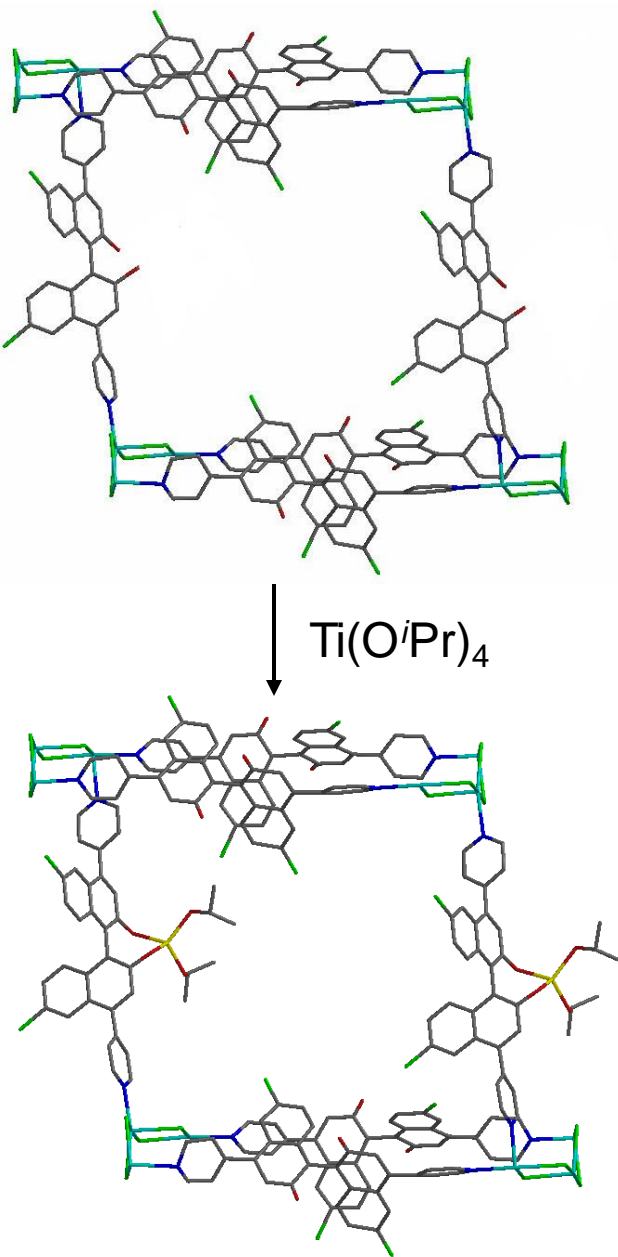
Synthesis of Chiral Lamellar Lanthanide Phosphonate MOFs



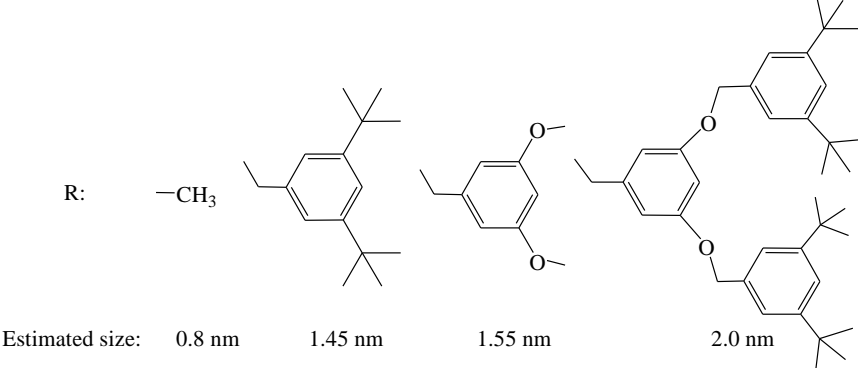
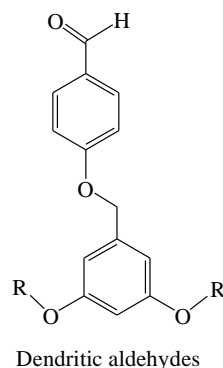
Single-Crystalline MOF for Asymmetric Diethylzinc Additions



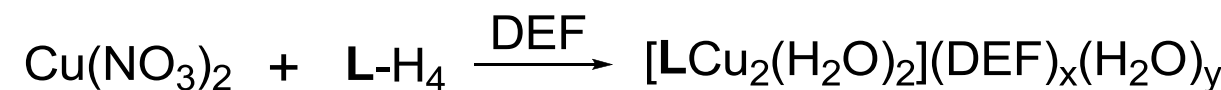
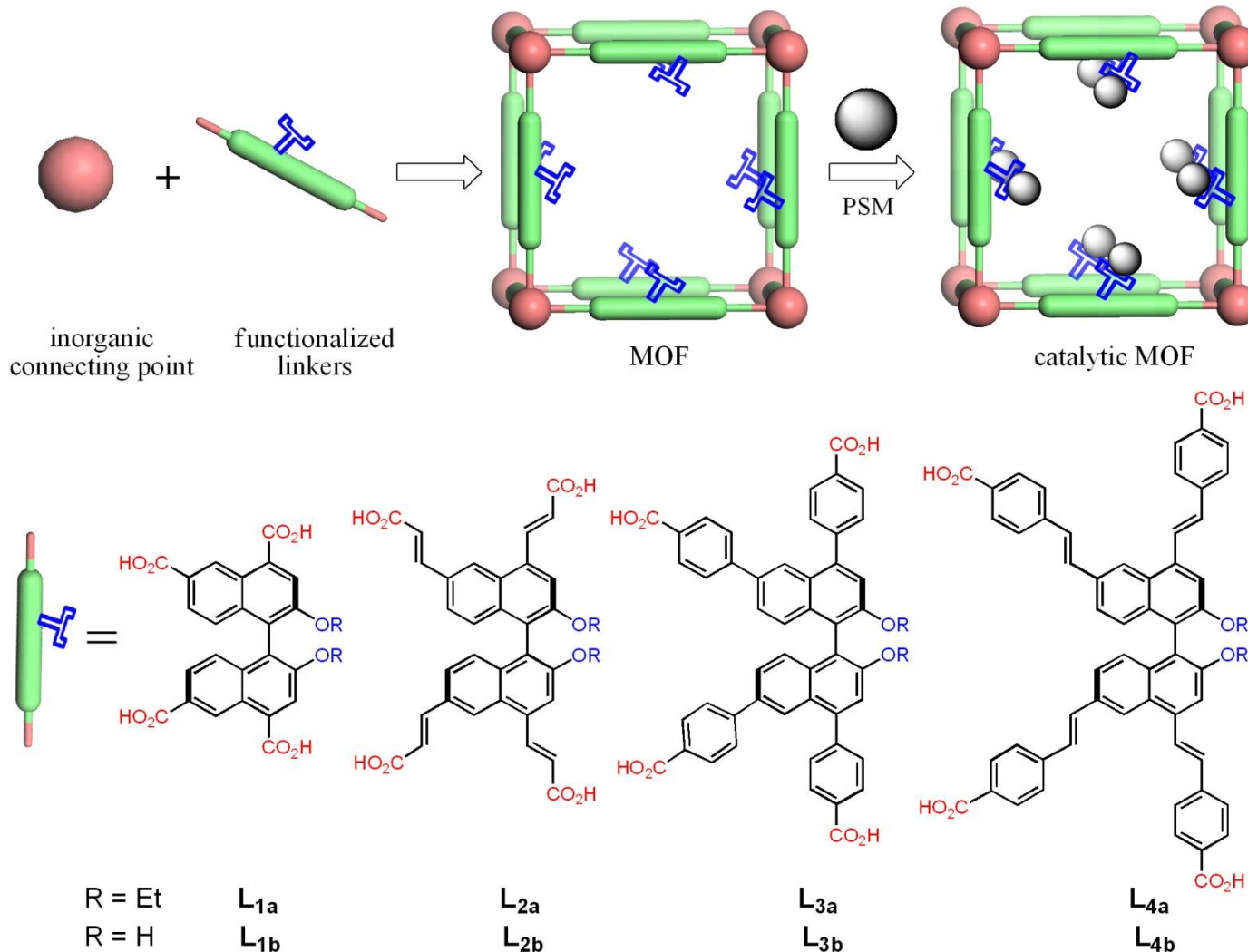
Single-Crystalline MOF for Asymmetric Diethylzinc Additions



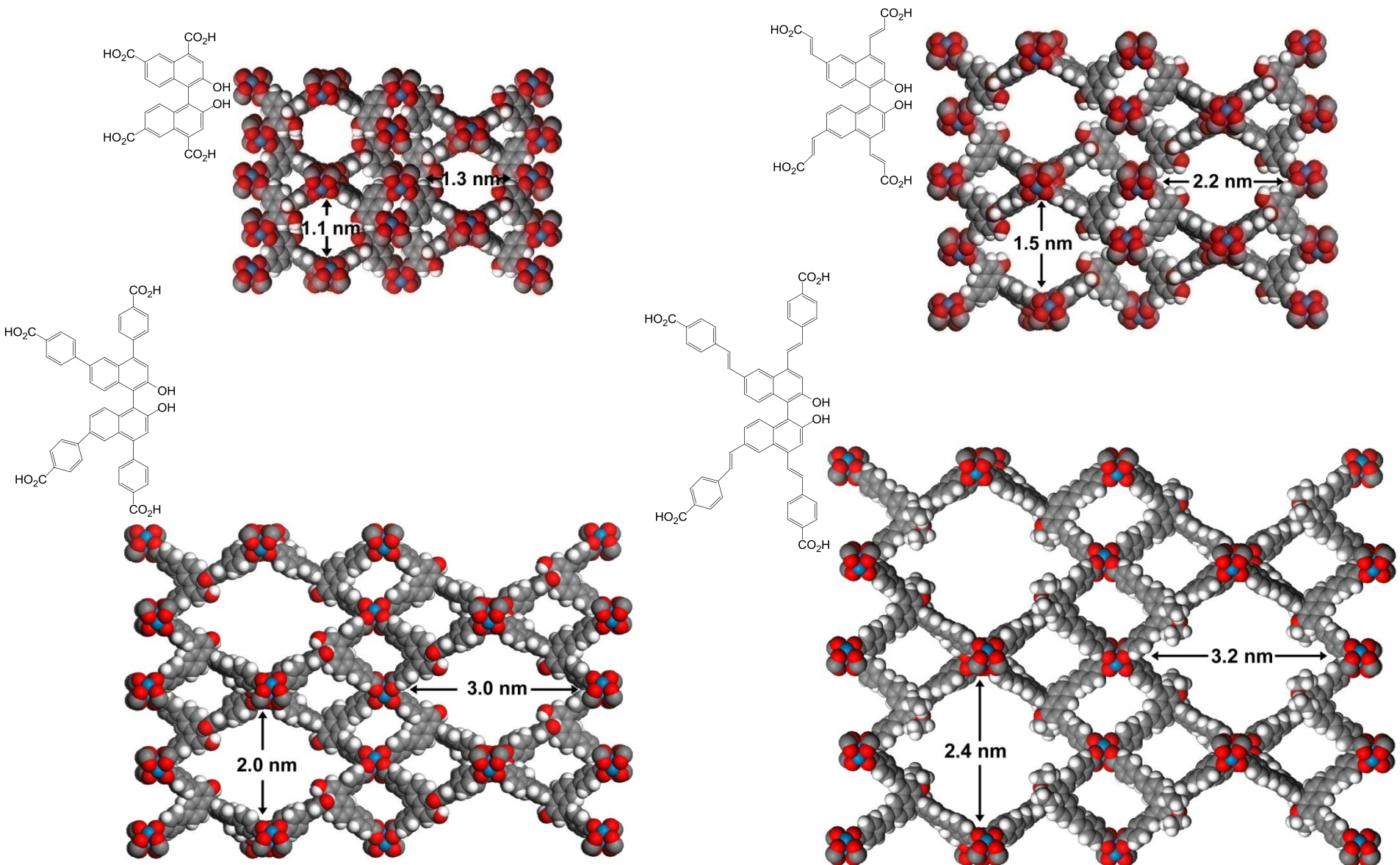
Ar	BINOL/ $\text{Ti}(\text{O}^{\prime}\text{Pr})_4$		1•Ti	
	conv.%	ee%	conv.%	ee%
1-Naph	>99	94	>99	93
Ph	>99	88	>99	83
4-Cl-Ph	>99	86	>99	80
3-Br-Ph	>99	84	>99	80
4'-G ₀ OPh	>99	80	>99	88
4'-G ₁ 'OPh	>99	75	73	77
4'-G ₁ OPh	>99	78	63	81
4'-G ₂ 'OPh	95 ^b	67 ^b	0	—



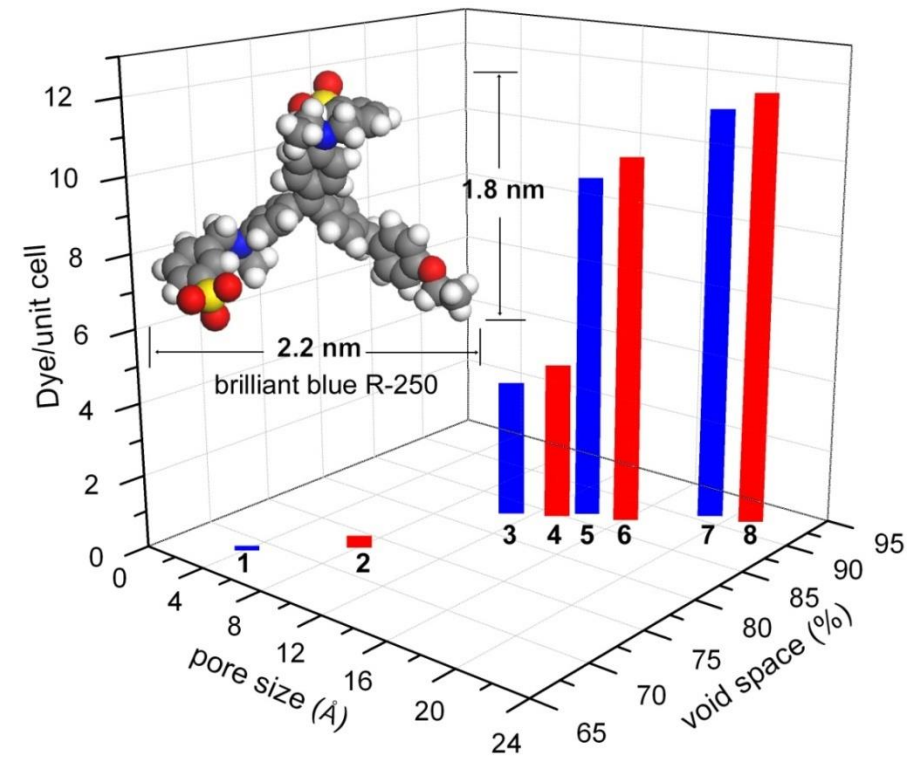
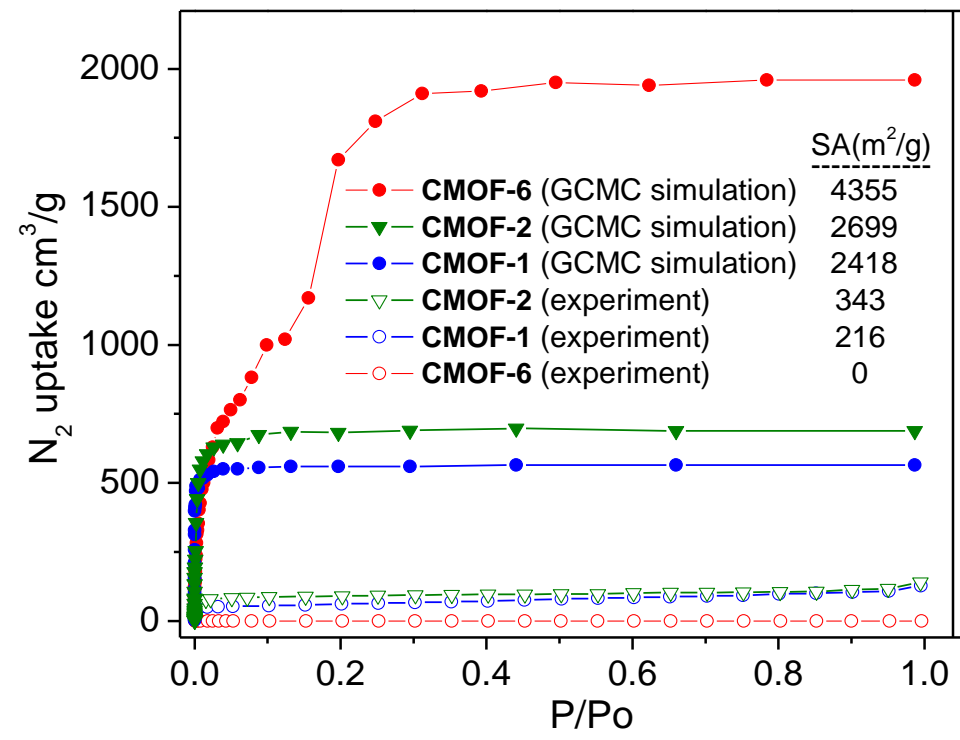
Isoreticular Homochiral Frameworks



Isoreticular Homochiral Frameworks Viewed along the *a* Axis

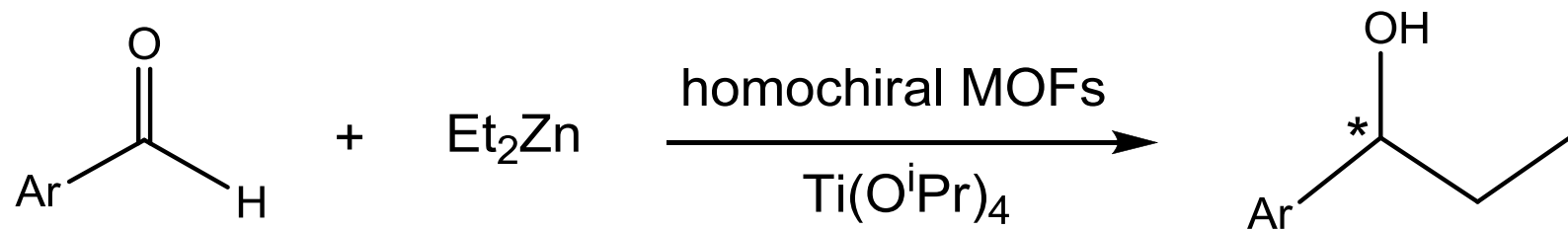


Severe Framework Distortion Upon Solvent Removal



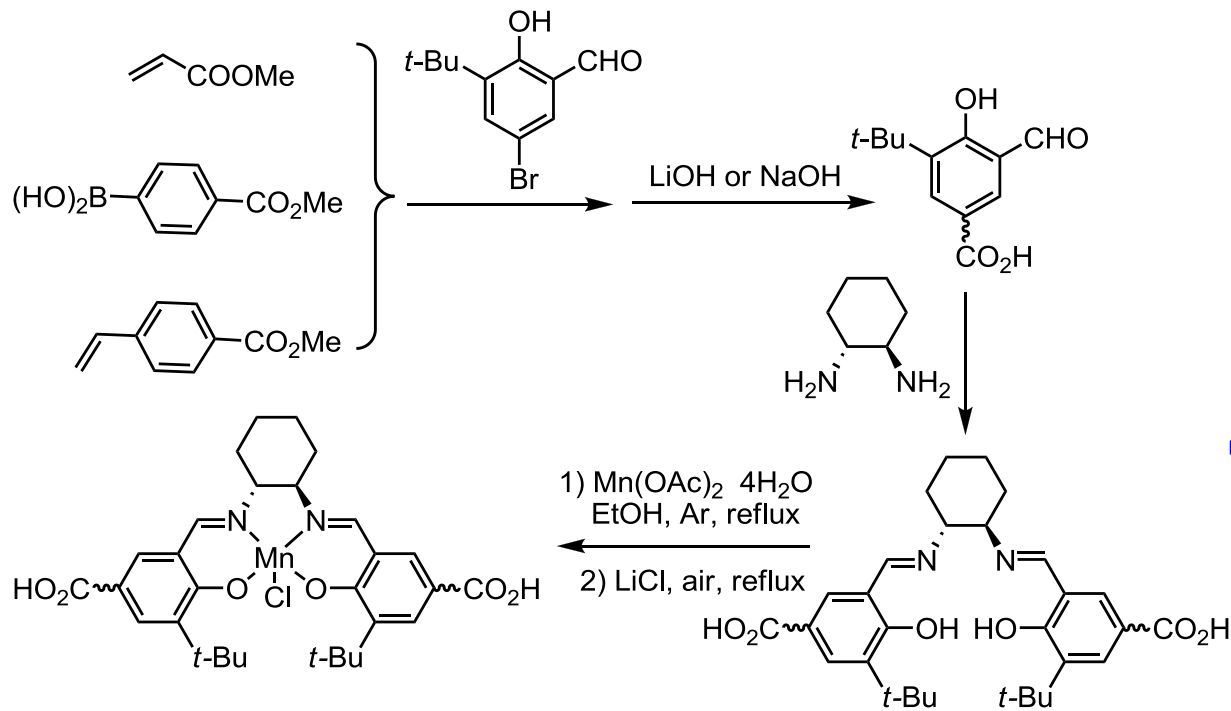
- “Permanent porosity” (from gas sorption measurements) does not provide an accurate description of catalytically active MOFs as large pore sizes and channels can lead to severe framework distortion upon solvent removal.
- “Permanent porosity” is not needed for heterogeneous catalysis since most of the catalytic reactions are carried out in the presence of solvents.

Catalytic Diethylzinc Addition as A Probe for Substrate Accessibility



Entry	CMOF-	Ar	Selectivity %	Conv. %	ee %
1	6	1-Naph	92	>99	91
2	6	4-Cl-Ph	84	>99	80
3	6	4-Br-Ph	53	93	80
4	6	4'-Me-Ph	72	>99	78
5	6	Ph	68	>99	82
6	8	Ph	82	>99	84
7	4	Ph	64	98	70
8	2	Ph	91	98	<3
9	5	Ph	10	>99	0

Isoreticular Salen-based MOFs

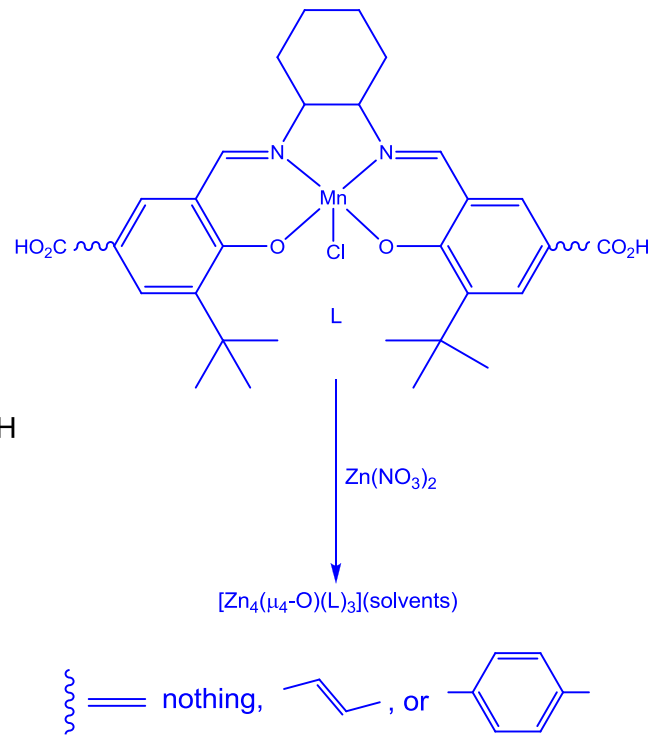


L1: $\sim\!\sim$ = nothing

L2: $\sim\!\sim$ = $\text{CH}_2=\text{CH}-$

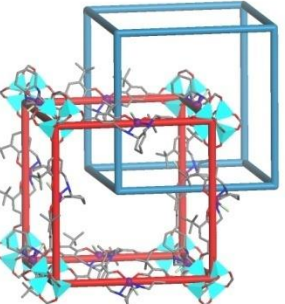
L3: $\sim\!\sim$ = C_6H_4-

L4: $\sim\!\sim$ = $\text{C}_6\text{H}_4-\text{CH}_2-$

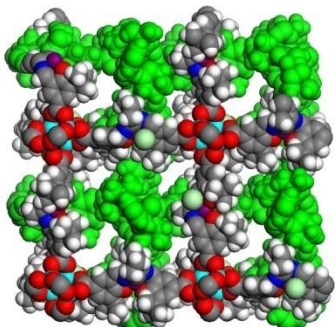


$\sim\!\sim$ = nothing, $\text{CH}_2=\text{CH}-$, or C_6H_4-

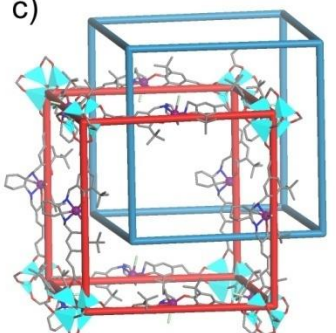
a)



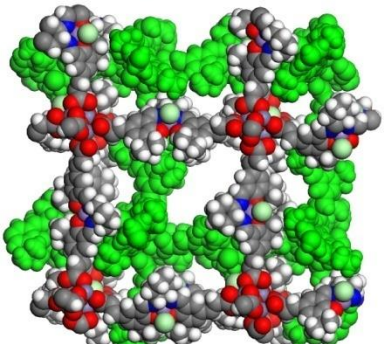
b)



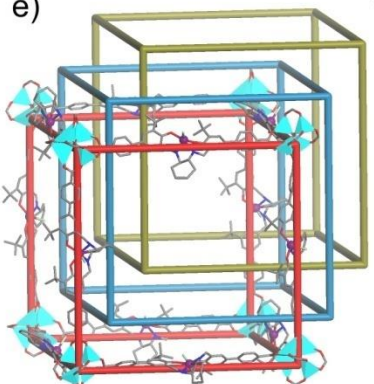
c)



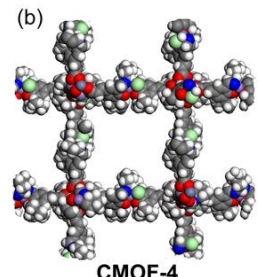
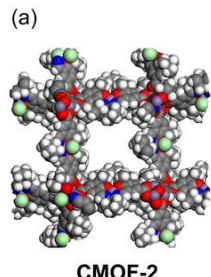
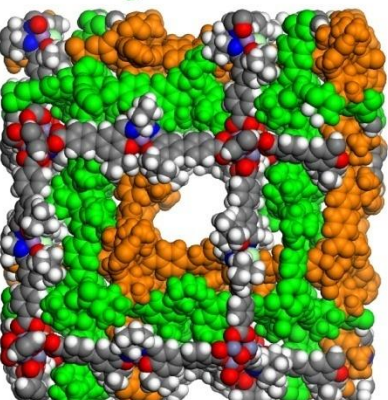
d)



e)

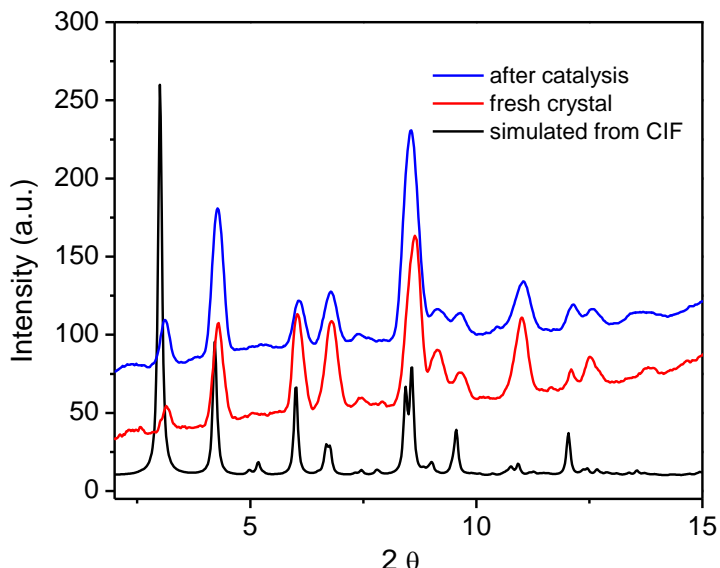
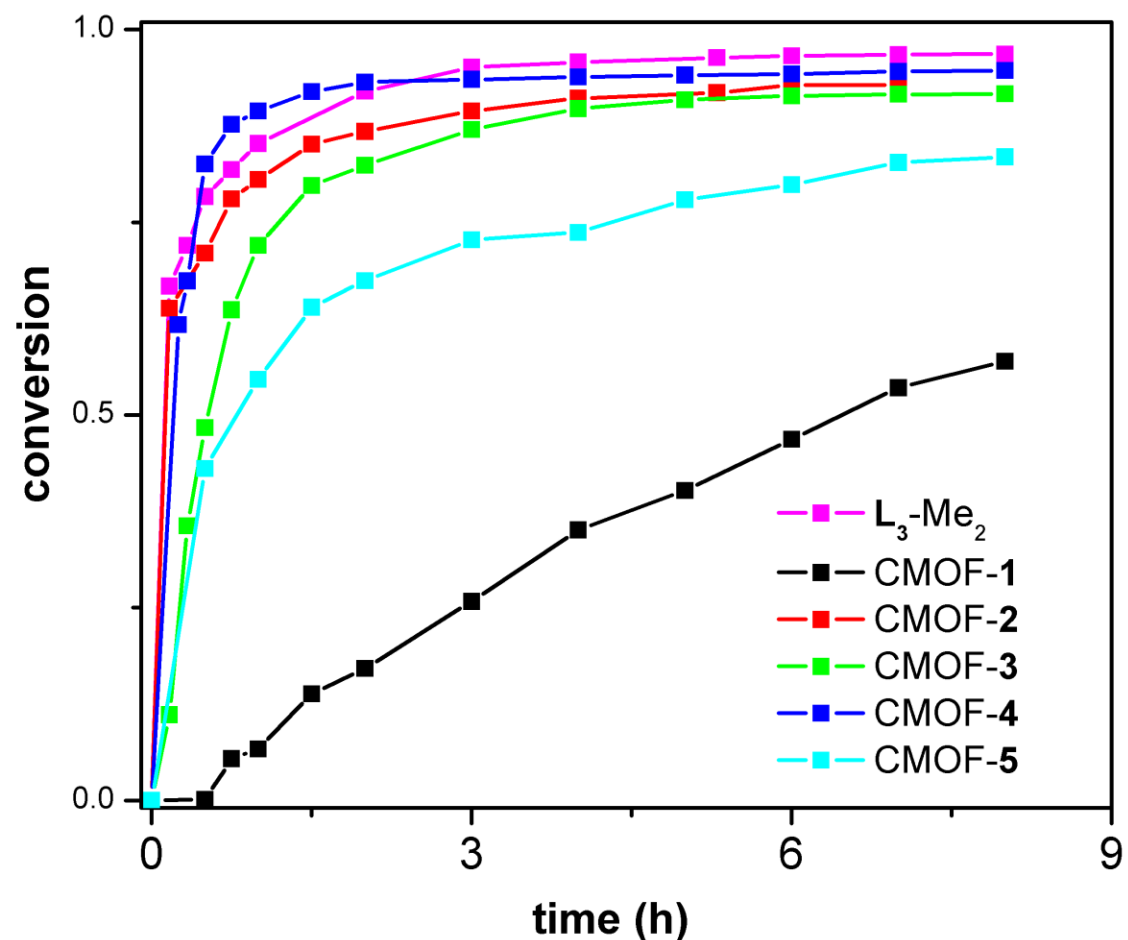
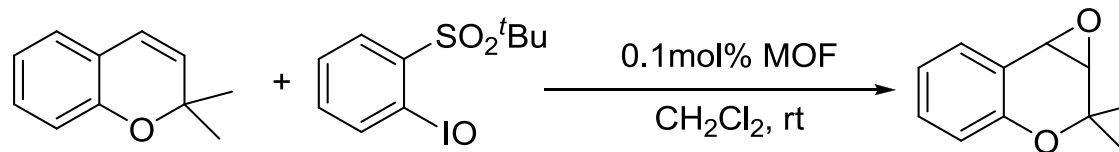


f)

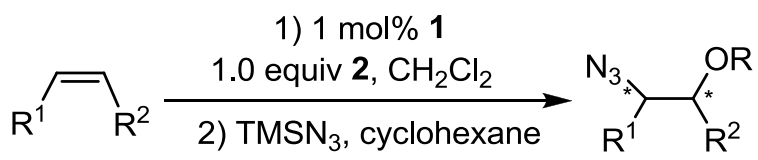
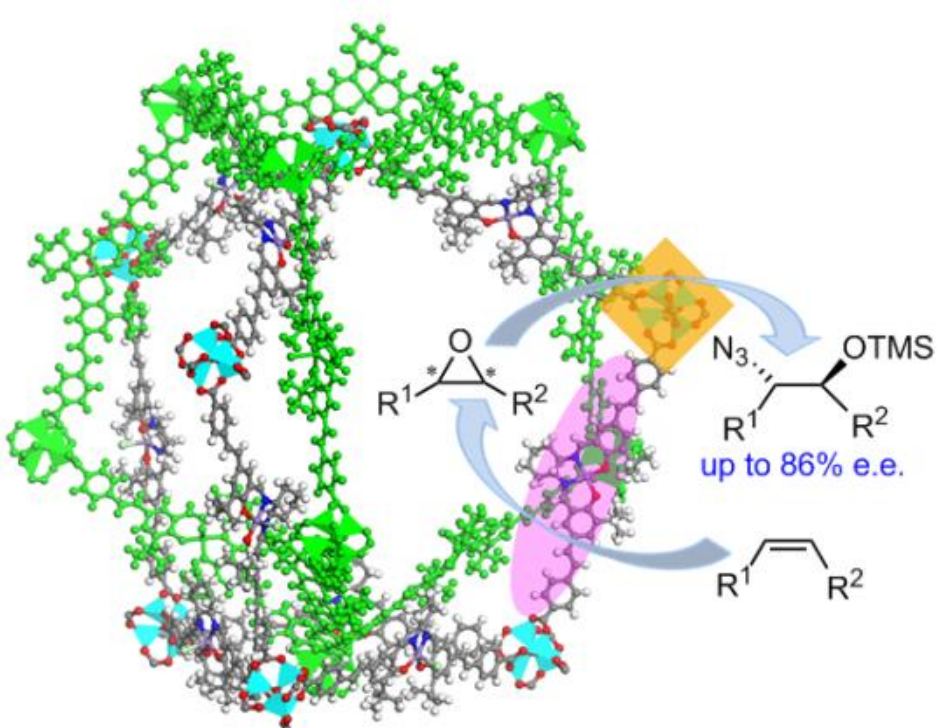
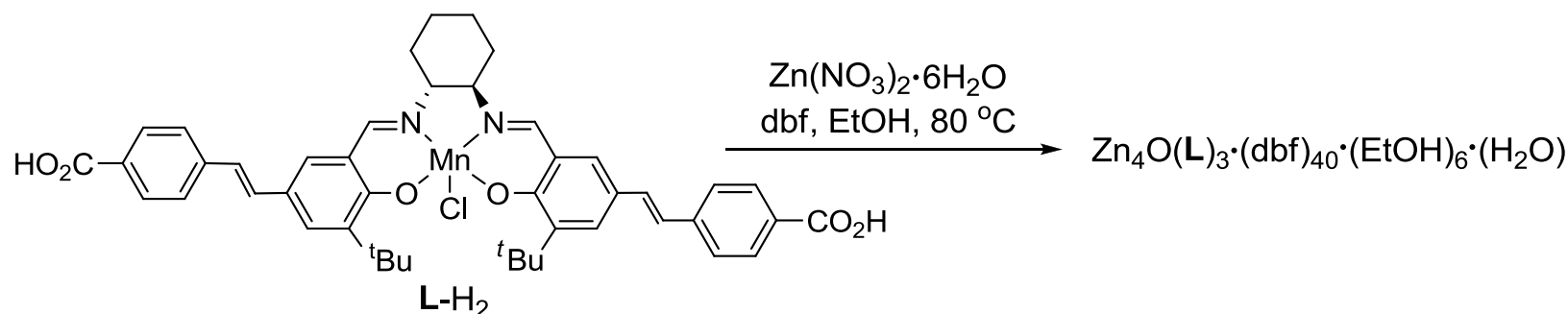


<chem>R1=CH2</chem>	<chem>R2=CH2</chem>	<chem>6a-g</chem>	<chem>7</chem>	$0.1 \text{ mol\% catalyst}$	$\text{CH}_2\text{Cl}_2, \text{ r.t.}$	<chem>*C1(*)C(O)C1R2</chem>
entry	catalyst		alkene	conv.% ^b	ee% ^c	
1	CMOF-1			63	47	
2	CMOF-3		<chem>6a</chem>	80	64	
3	CMOF-5		<chem>6a</chem>	54	61	
4	$\text{L}_3\text{-Me}_2$			60	64	
5	CMOF-5		<chem>6b</chem>	82	92	
6	CMOF-4		<chem>6b</chem>	87	85	
7	$\text{L}_3\text{-Me}_2$			90	92	
8	CMOF-5		<chem>6c</chem>	60	79	
9	CMOF-4		<chem>6c</chem>	79	83	
10	$\text{L}_3\text{-Me}_2$			82	88	
11	CMOF-4		<chem>6d</chem>	93	81	
12	$\text{L}_3\text{-Me}_2$			97	88	
13	CMOF-4		<chem>6e</chem>	89	77	
14	$\text{L}_3\text{-Me}_2$			80	87	
15	CMOF-4		<chem>6f</chem>	79	75	
16	$\text{L}_3\text{-Me}_2$			81	88	
17	CMOF-5		<chem>6g</chem>	>99	42	
18	CMOF-4		<chem>6g</chem>	>99	39	
19	$\text{L}_3\text{-Me}_2$			>99	45	

Expoxidation Rates Depend on MOF Channel Sizes

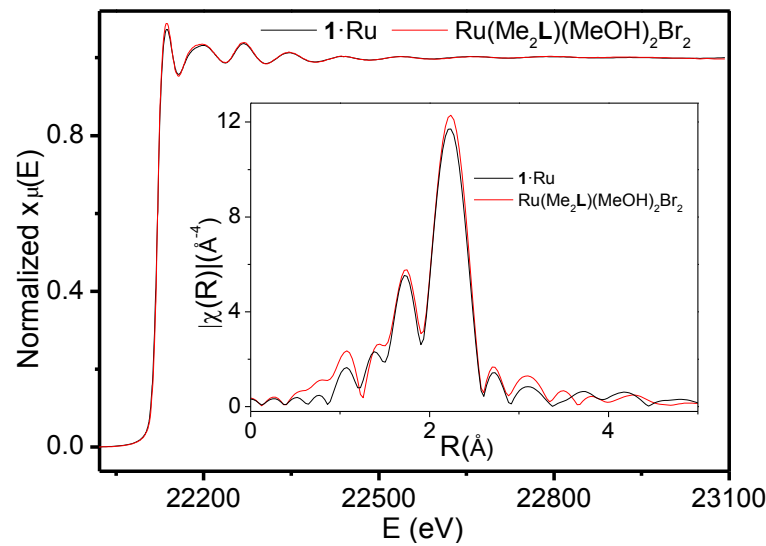
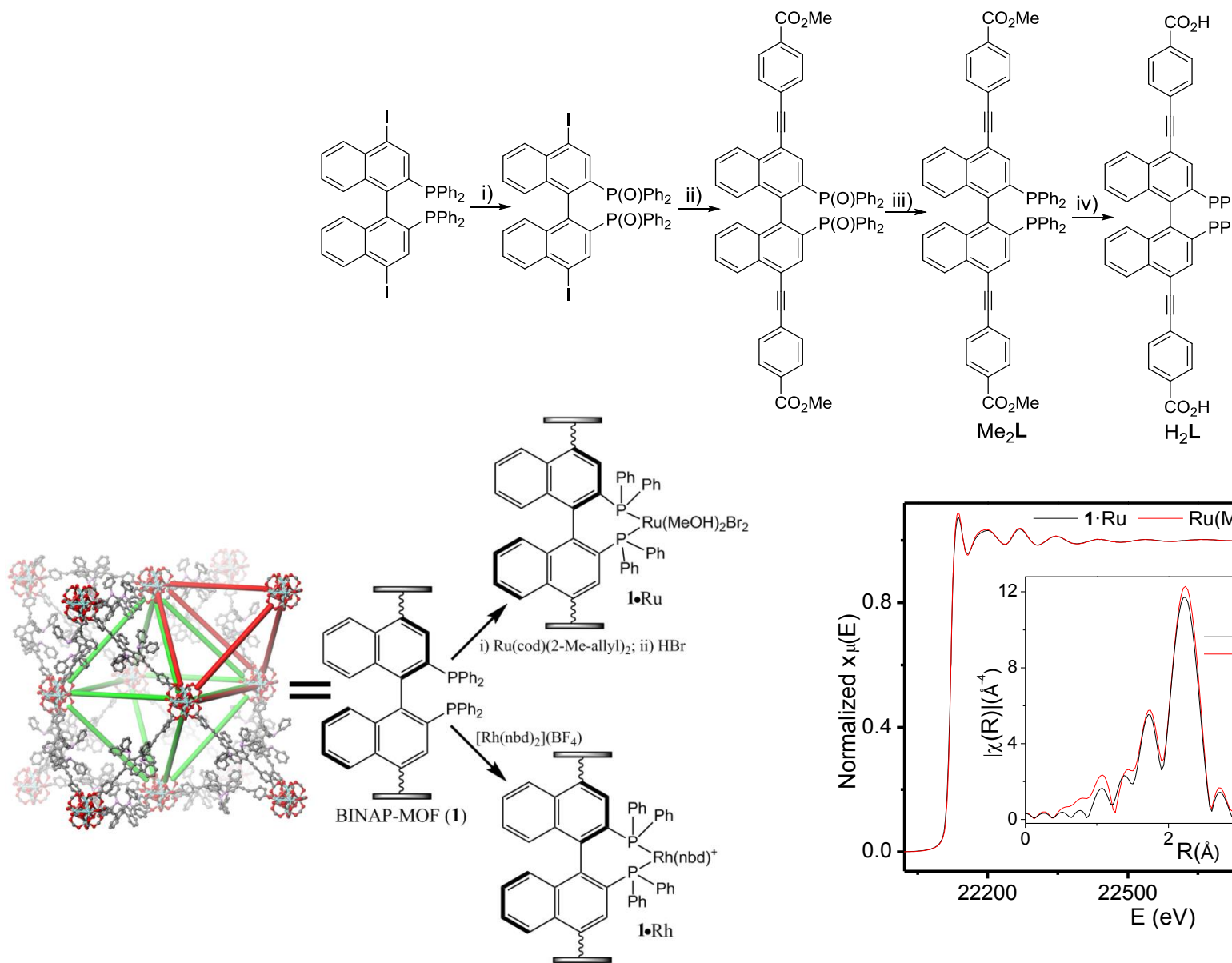


MOF-catalyzed sequential asymmetric epoxidation/ring-opening reactions

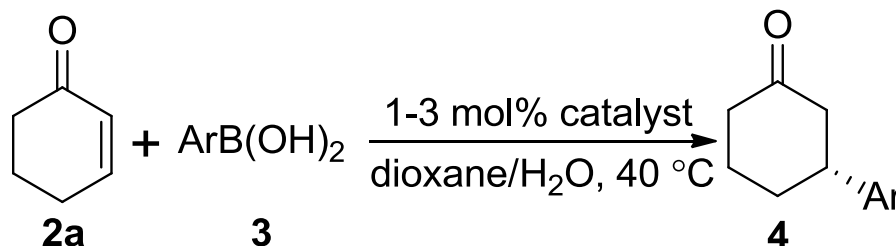


Substrate	Product	Yield[%]	ee[%]
3d	$\text{MeO}-\text{C}_6\text{H}_3-\text{CH}(\text{N}_3)-\text{CH}_2-\text{CH}(\text{OH})-\text{CH}_2-\text{C}_6\text{H}_3-\text{O}-\text{CH}_2$ (5a)	57	81 (82)
3g	$\text{C}_6\text{H}_5-\text{C}_4\text{H}_3-\text{CH}(\text{N}_3)-\text{CH}_2-\text{OTMS}$ (5b)	60	50 (48)

Privileged Phosphine-Based Metal-Organic Frameworks for Broad-Scope Asymmetric Catalysis

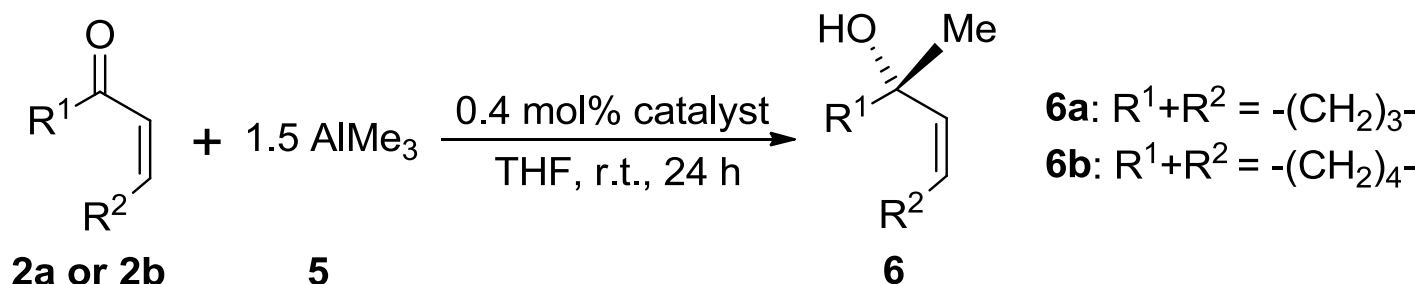


Privileged Phosphine-Based Metal-Organic Frameworks for Broad-Scope Asymmetric Catalysis

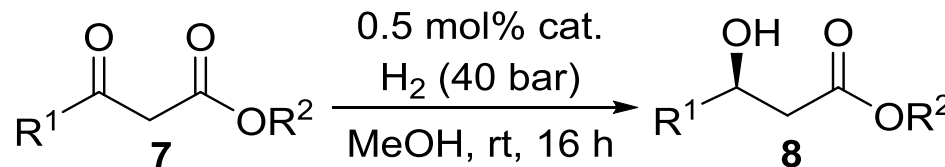


entry	Ar	catalyst	loading	yield	e.e.%
1	Ph	$1\bullet\text{Rh}$	1 mol%	80%	>99
2	m-MeCO ₂ Ph	$1\bullet\text{Rh}$	1 mol%	85%	>99
3	p-MeC(O)-Ph	$1\bullet\text{Rh}$	1 mol%	99%	99
4	Ph	Rh-H ₂ L	3 mol%	0%	N/A
5	Ph	Rh-Me ₂ L	3 mol%	7% ^d	N/A
6	Ph	Rh-BINAP	1 mol%	29%	>99
7	m-MeCO ₂ Ph	Rh-BINAP	1 mol%	34%	>99
8	p-MeC(O)-Ph	Rh-BINAP	1 mol%	46%	>99
9	Ph	Rh-BINAP	3 mol%	85%	>99
10	m-MeCO ₂ Ph	Rh-BINAP	3 mol%	87%	99
11	p-MeC(O)-Ph	Rh-BINAP	3 mol%	87%	>99

Privileged Phosphine-Based Metal-Organic Frameworks for Broad-Scope Asymmetric Catalysis

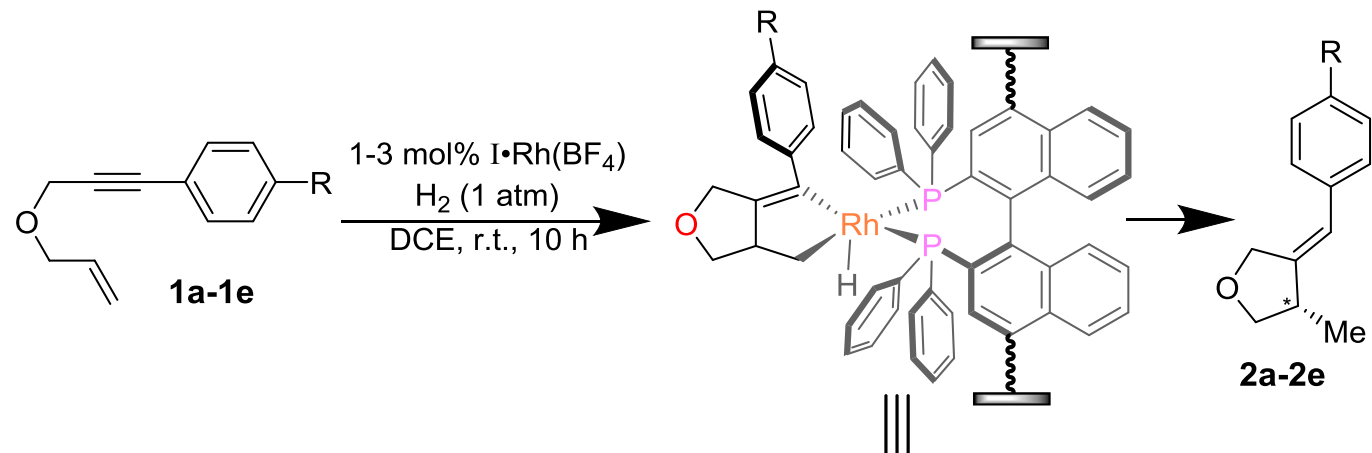


entry	substrate	catalyst	conv.% ^a	e.e.% ^a	yield ^b
1		1•Rh	97	98	71%
2		Rh-Me ₂ L	82	>99	46%
3		1•Rh	97	99	68%
4		Rh-Me ₂ L	91	>99	<40%

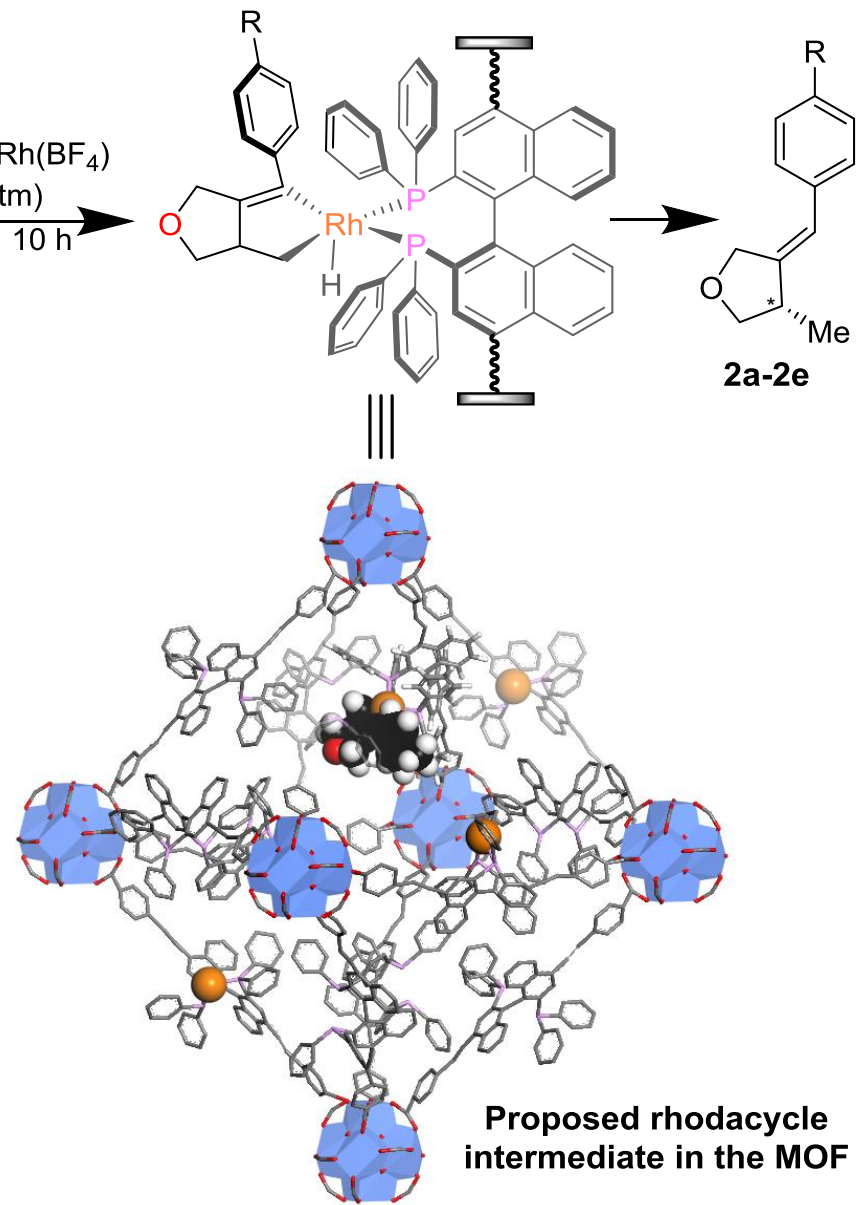


Quant. Conversion
Up to 97% ee

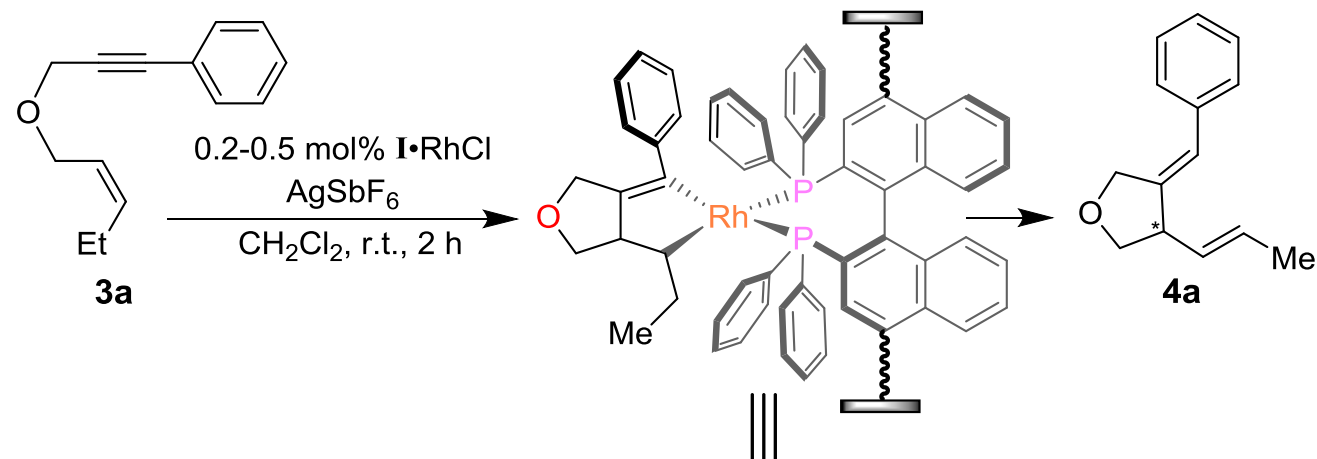
Privileged Phosphine-Based Metal-Organic Frameworks for Broad-Scope Asymmetric Catalysis



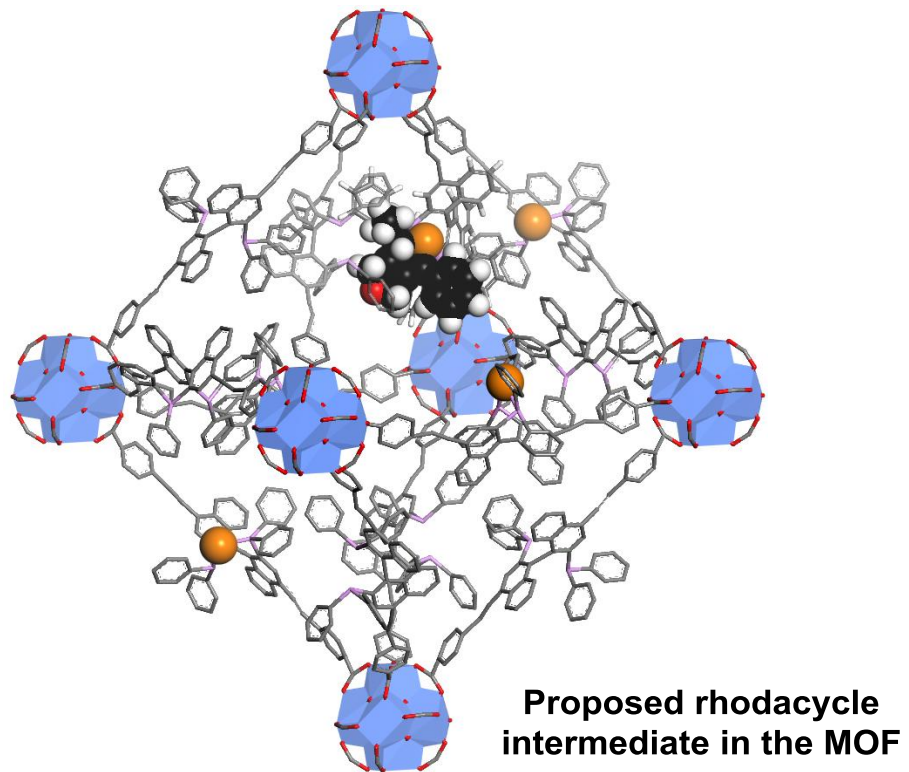
catalyst	R	Rh-loading (mol%)	yield (%) ^b	ee (%) ^c
I•Rh(BF₄)	Me (1a)	1	68	94
Rh(Me₂L1)BF₄	Me (1a)	1	10	91
I•Rh(BF₄)	Me (1a)	3	95	95
I•Rh(BF₄)	H (1b)	3	89	96
I•Rh(BF₄)	OMe (1c)	3	87	95
I•Rh(BF₄)	tBu (1d)	3	82	99
I•Rh(BF₄)	CF ₃ (1e)	3	70	94



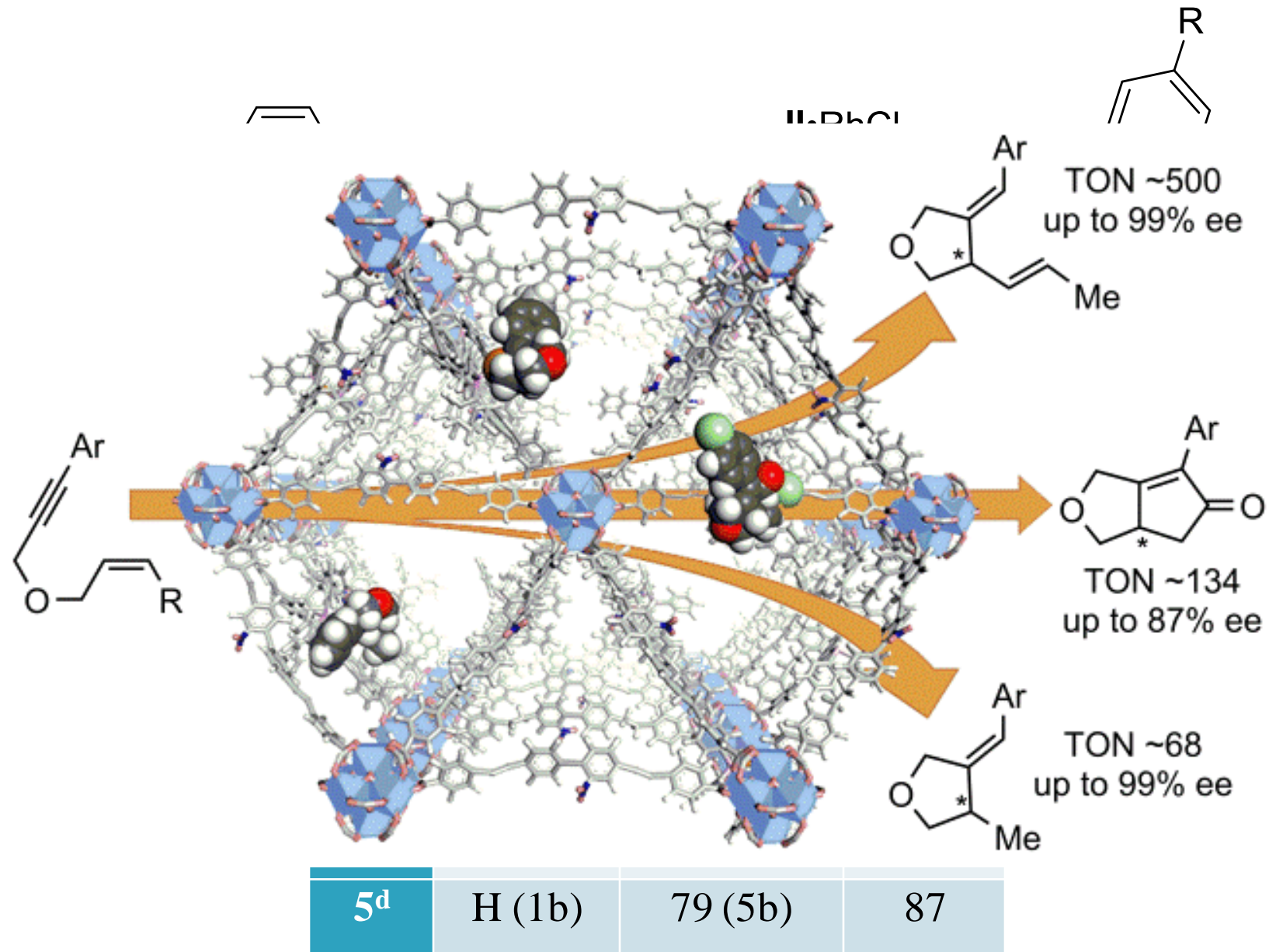
Privileged Phosphine-Based Metal-Organic Frameworks for Broad-Scope Asymmetric Catalysis



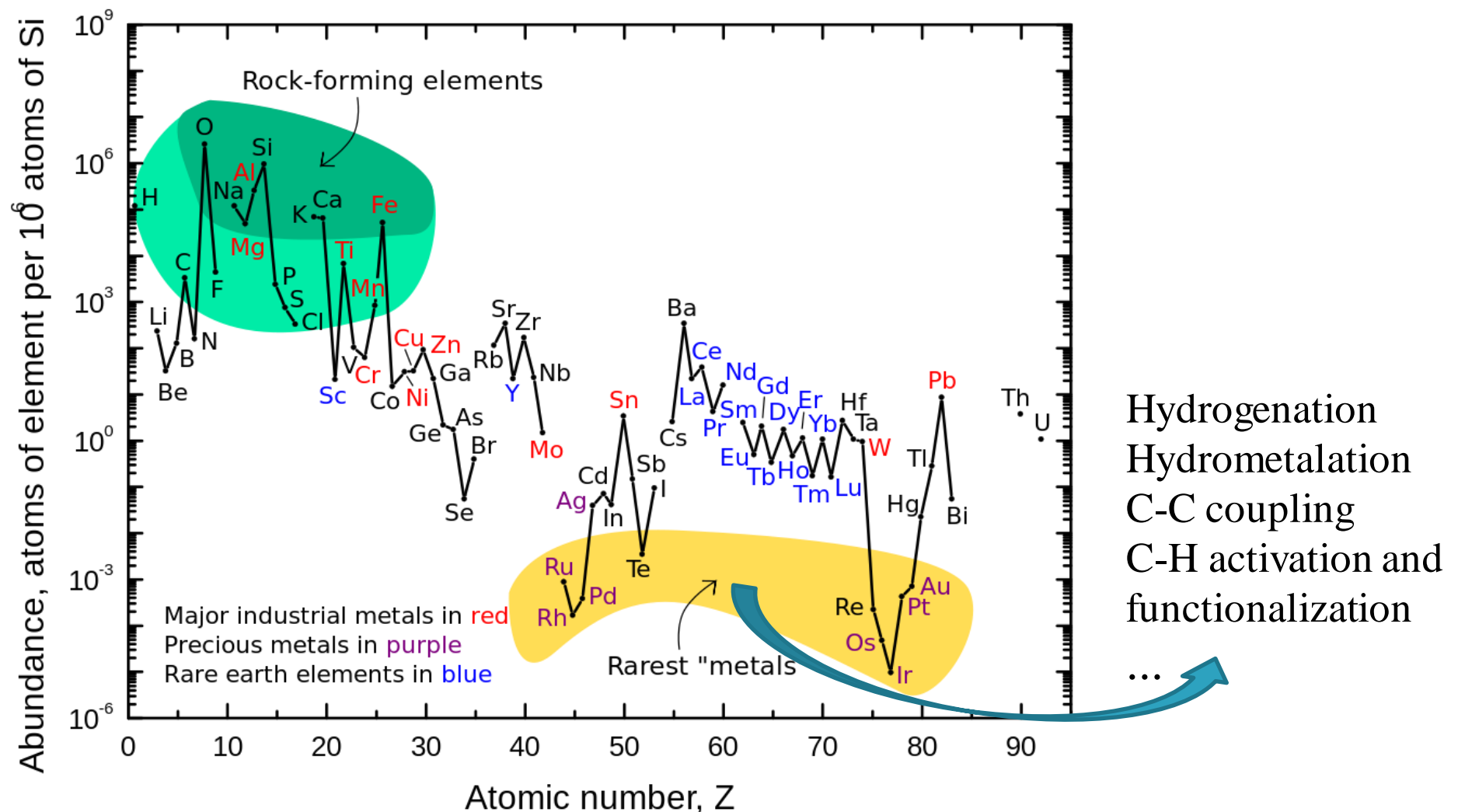
R	Rh loading (mol%)	yield (%) ^b	ee (%) ^c
H (3a)	0.2	99 (4a)	99
Me (3b)	0.2	65 (4b)	99
Me (3b)	0.5	99 (4b)	99
OMe(3c)	0.2	60 (4c)	99
OMe (3c)	0.5	99 (4c)	99
tBu (3d)	0.5	99 (4d)	99
CF ₃ (3e)	0.2	99 (4e)	99



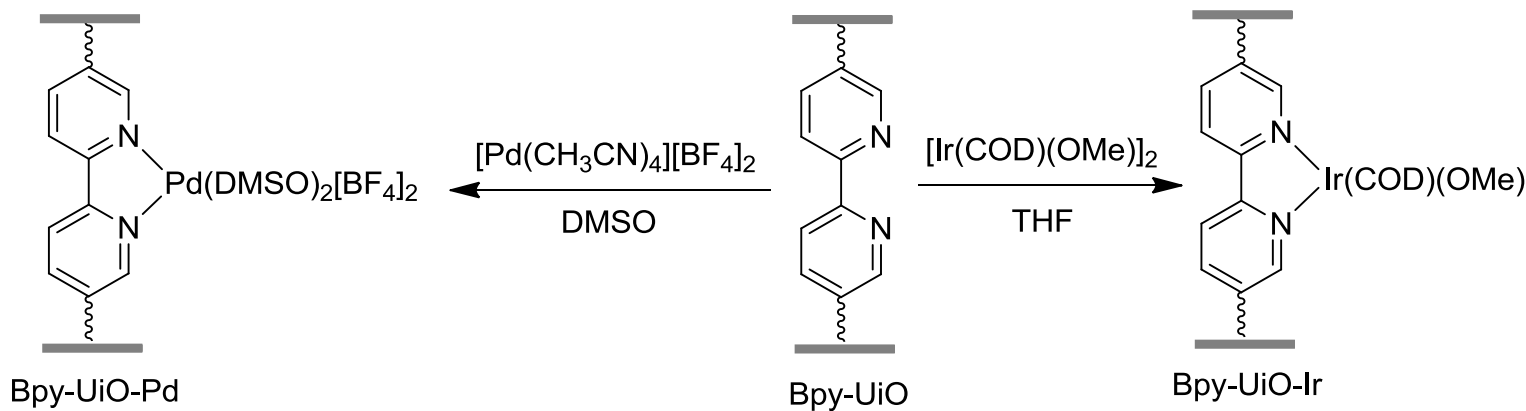
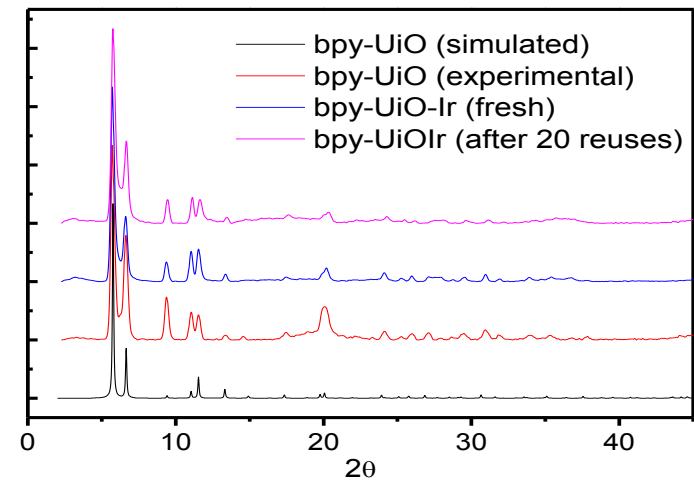
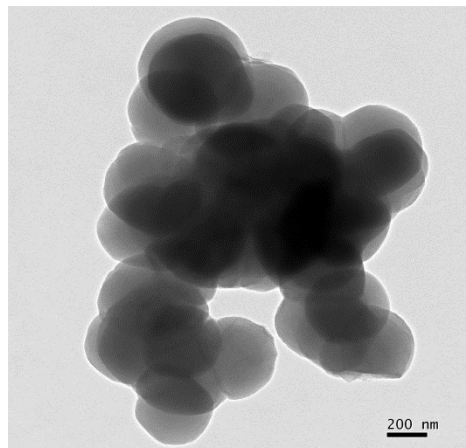
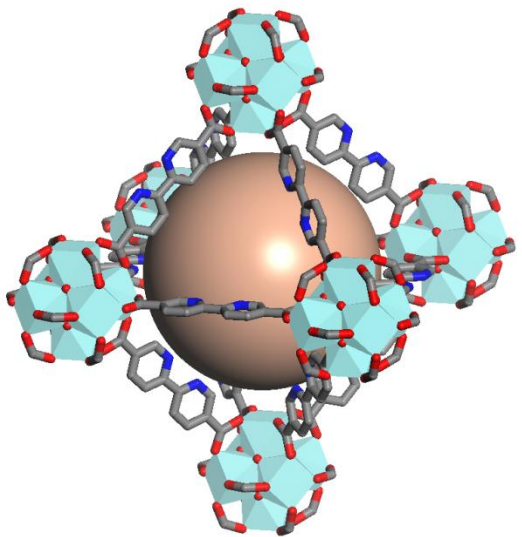
Mixed-Ligand MOFs for Asymmetric Pauson-Khand Reactions



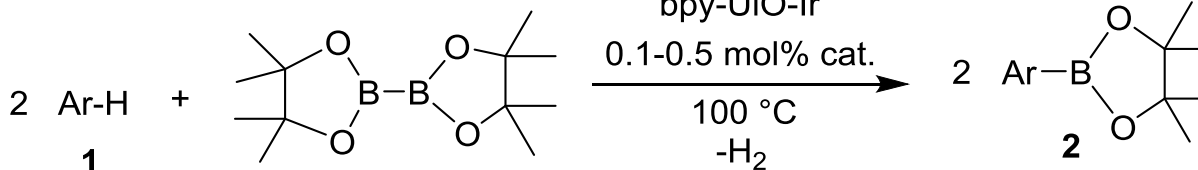
Many Industrial Catalysts Rely Metals of Low Abundance on Planet Earth



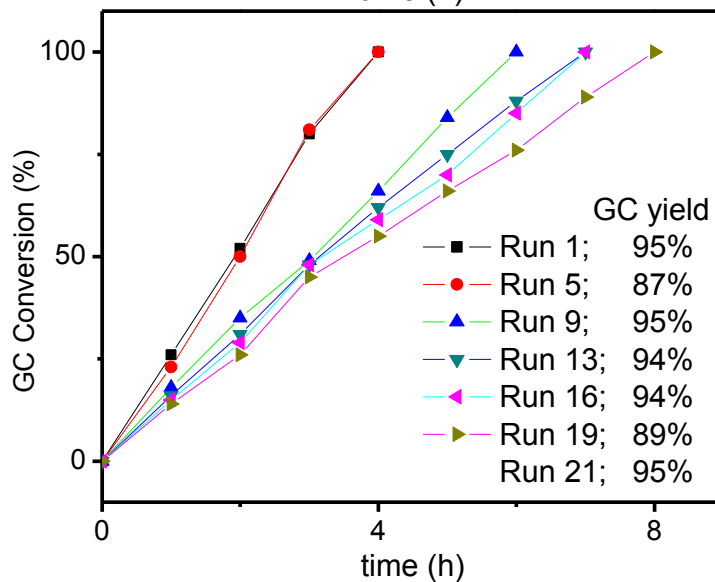
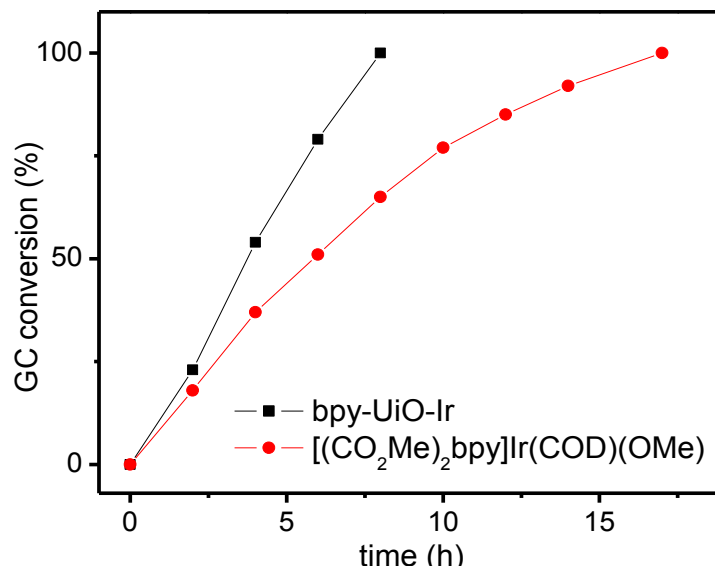
Bipyridyl-containing Metal-organic Frameworks for Highly Efficient Catalytic Organic Transformations



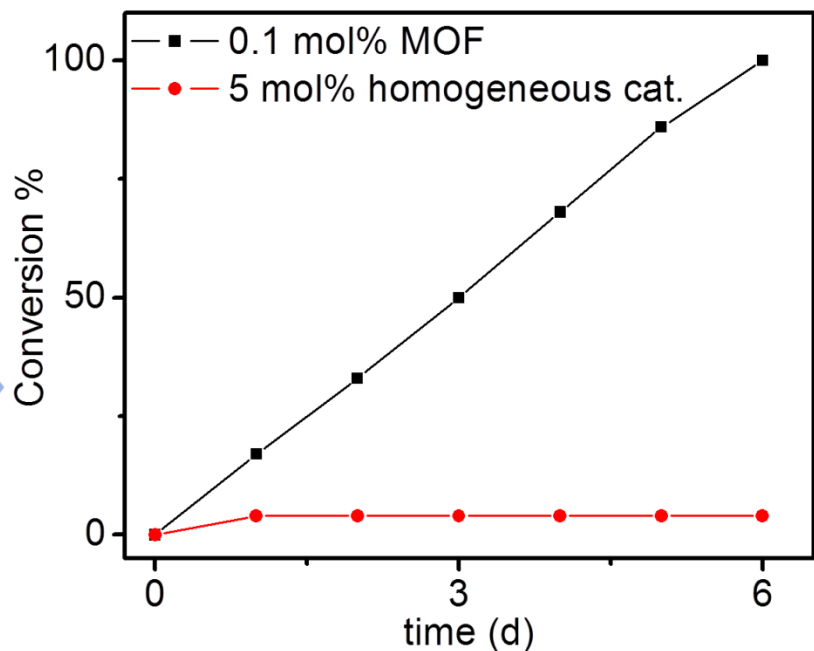
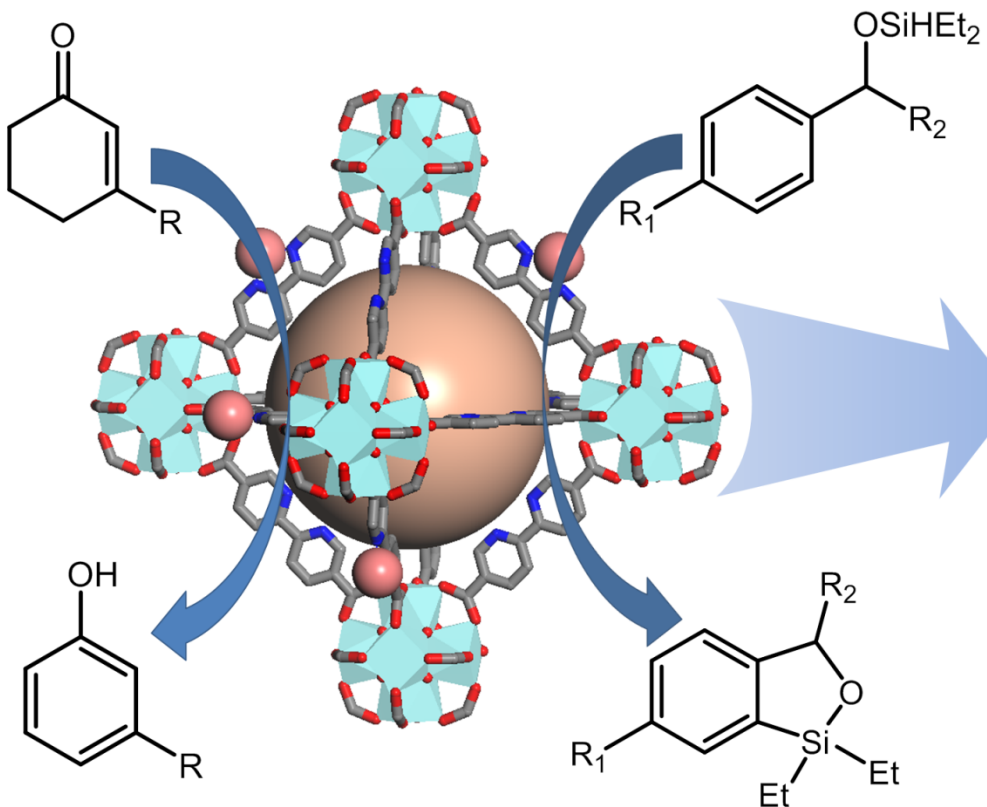
Bipyridyl-containing Metal-organic Frameworks for Arene Borylation



Entry	Arene	Product	Time	Isolated Yield (%)
1			28 h	85
2			4 d	83 ^b
3			12 h	86
4			10 h	93
5 ^c			9 h	96
6 ^c			4 d	96 ^b
7 ^c			7 h	94
8 ^c			8 h	93
9 ^c			4 d	95 ^b
10			17 h	91
11 ^c			15 h $(o:m:p = 0:60:40)$	93

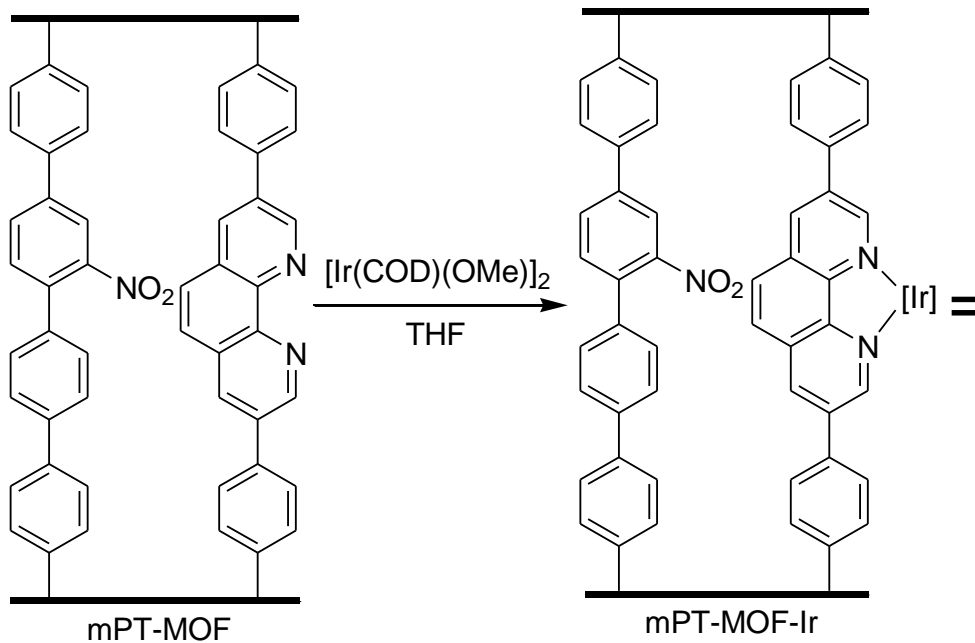
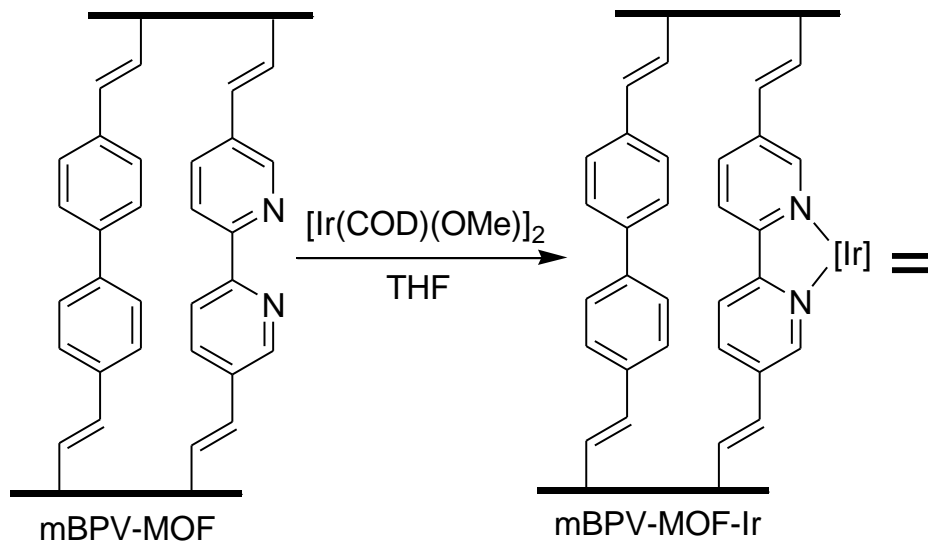


Bipyridyl-containing Metal-organic Frameworks for Silylation and Oxidation Reactions

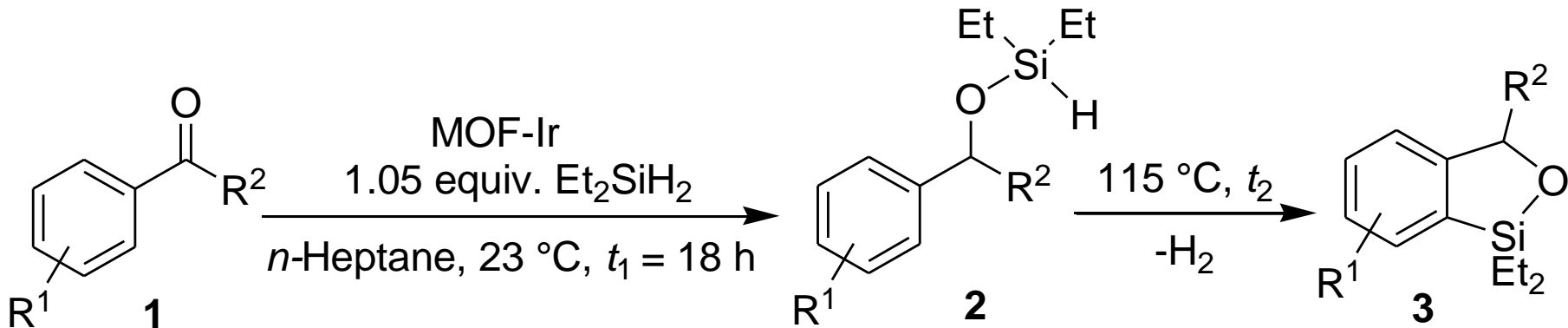


MOF is >1250 times more active than the homogeneous catalyst.

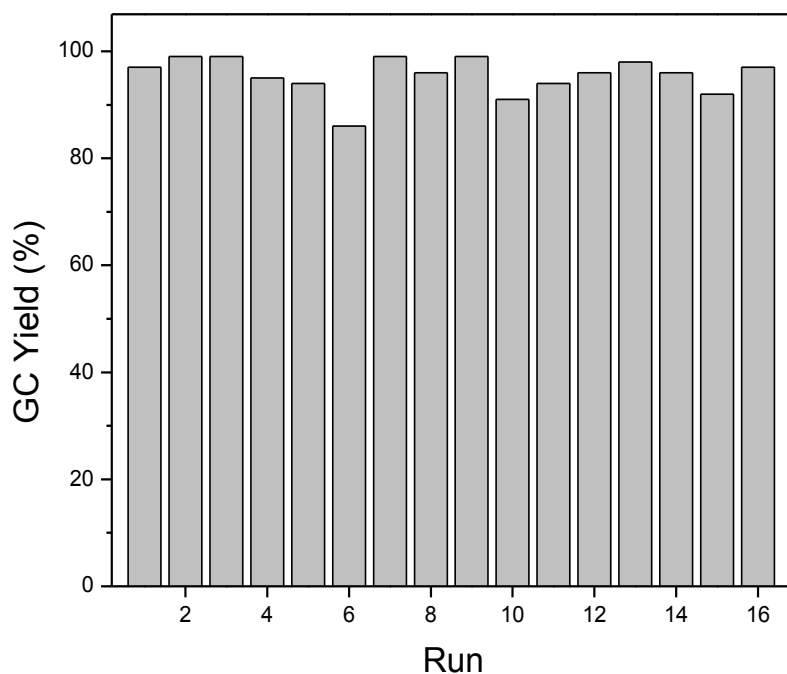
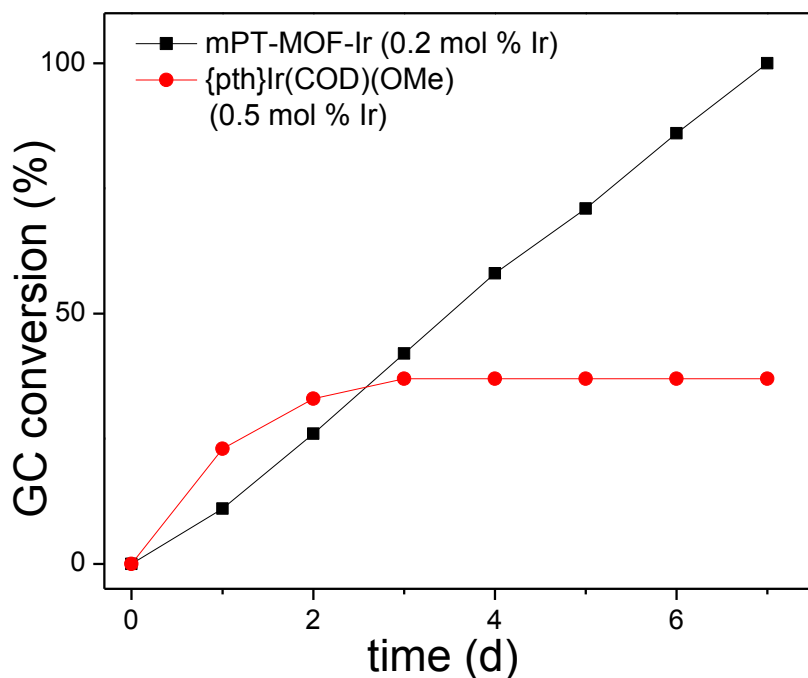
Mixed-Linker Metal-organic Frameworks Directed C-H Functionalization



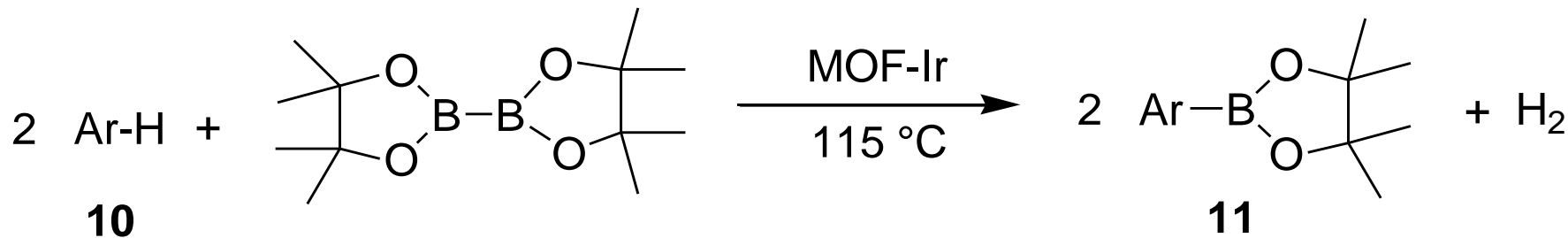
Mixed-Linker MOFs for Tandem Hydrosilylation and *ortho*-Silylation



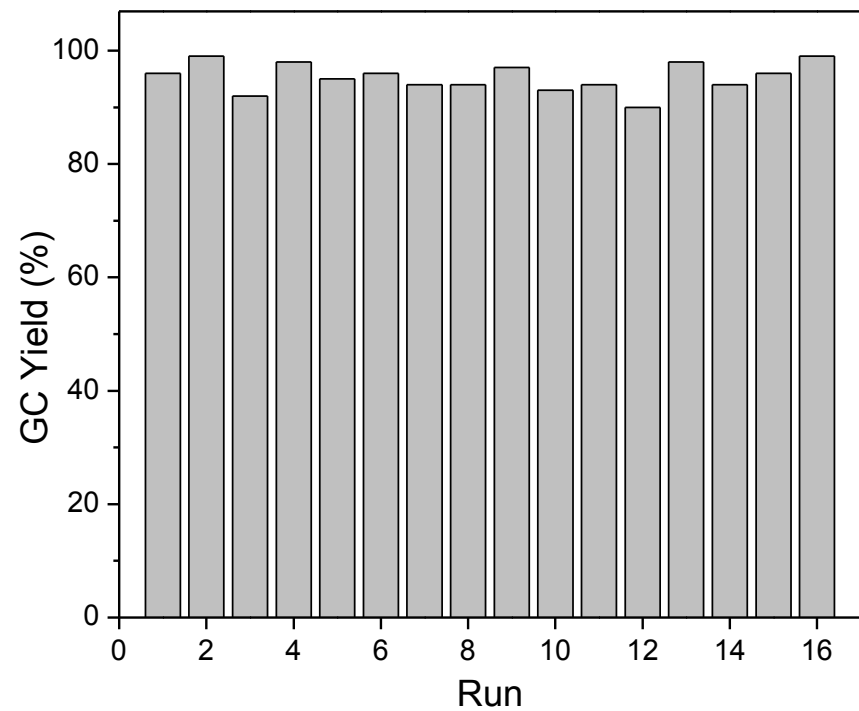
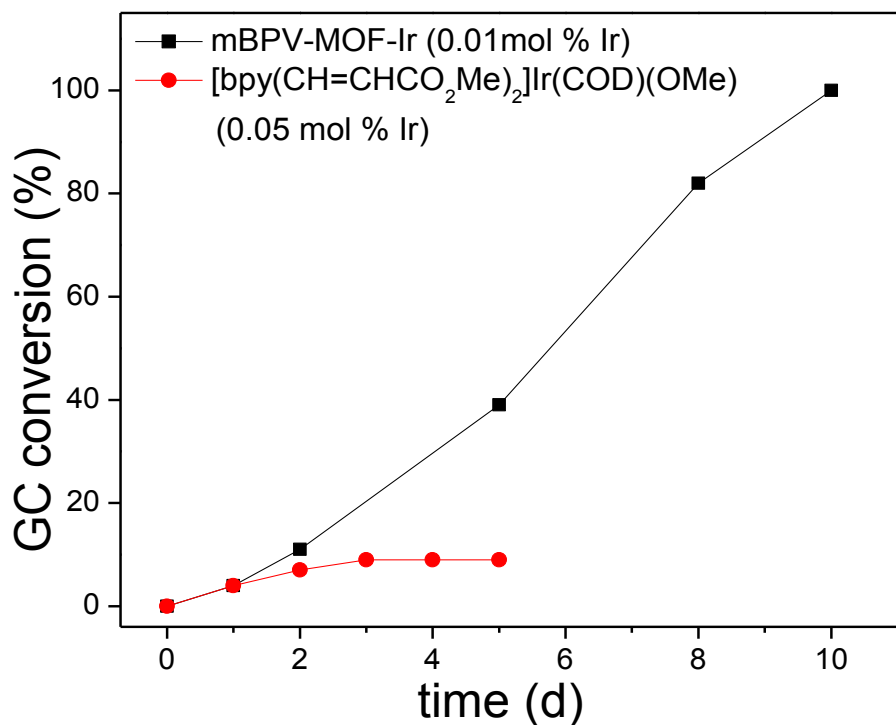
Broad substrate scope, TON ≥ 3040



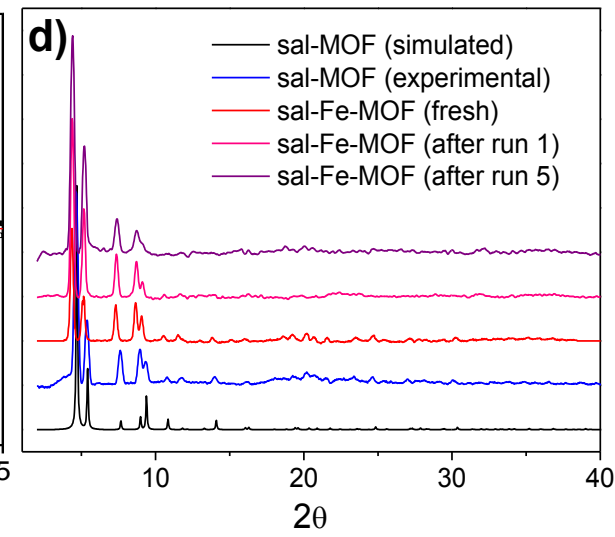
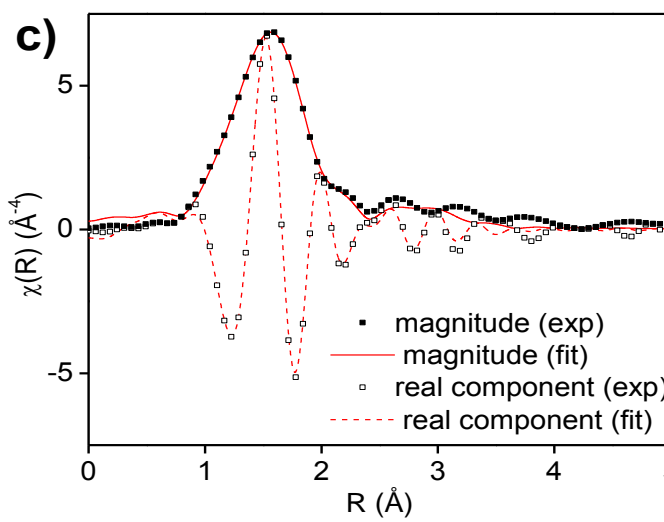
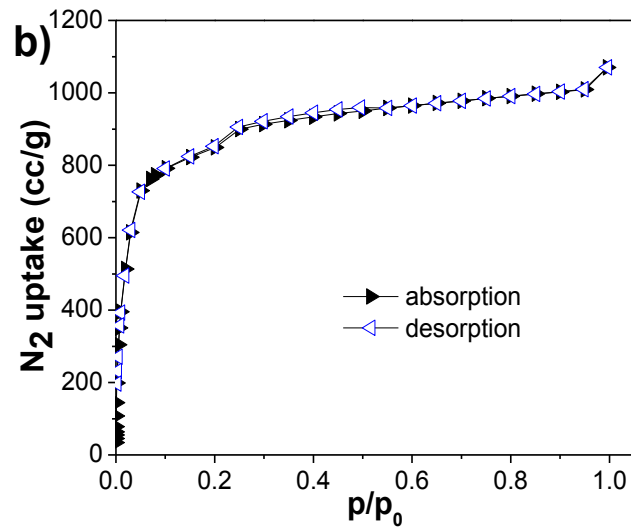
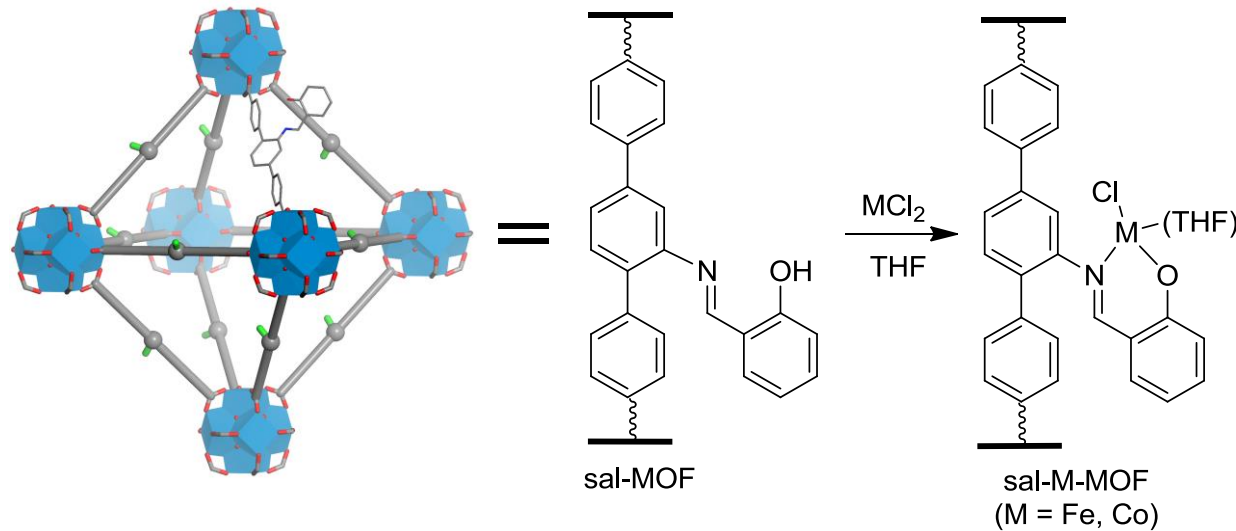
Mixed-Linker MOFs for C-H Borylation of Arenes



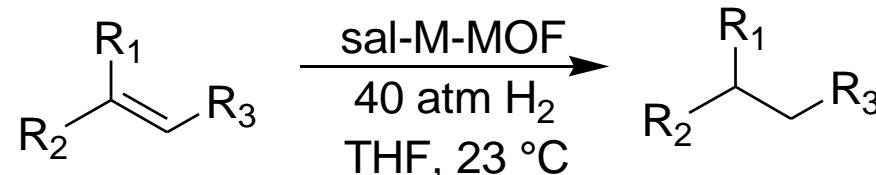
Broad substrate scope, TON $\geq 17,000$



A Salicylaldimine MOF Enables Highly Active Olefin Hydrogenation with Iron and Cobalt Catalysts

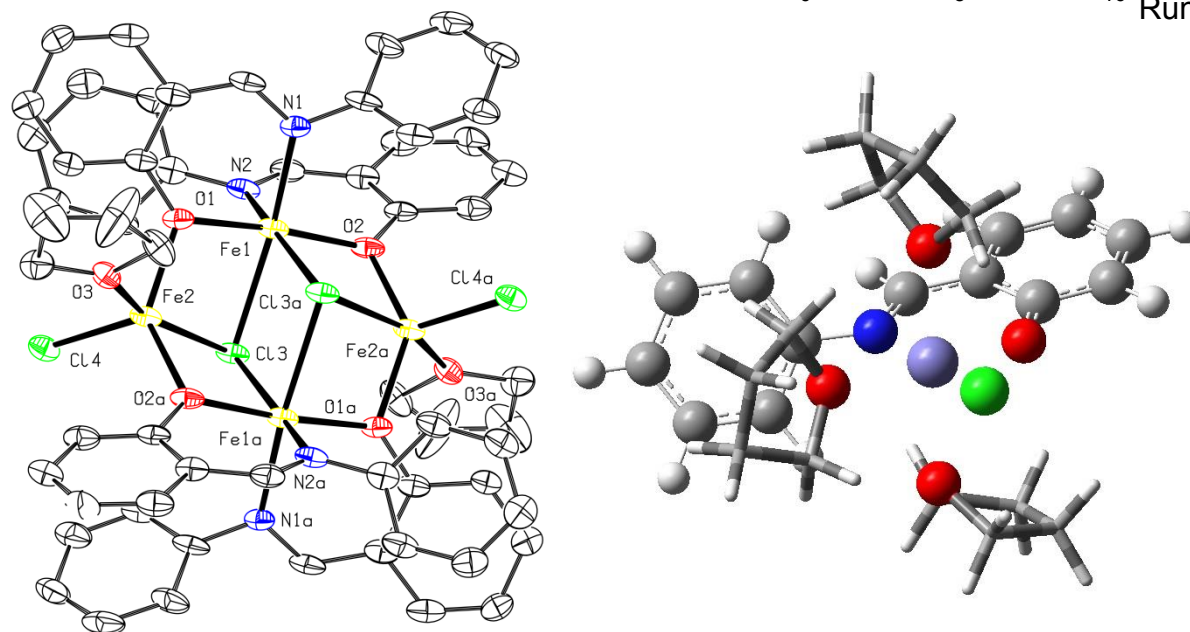
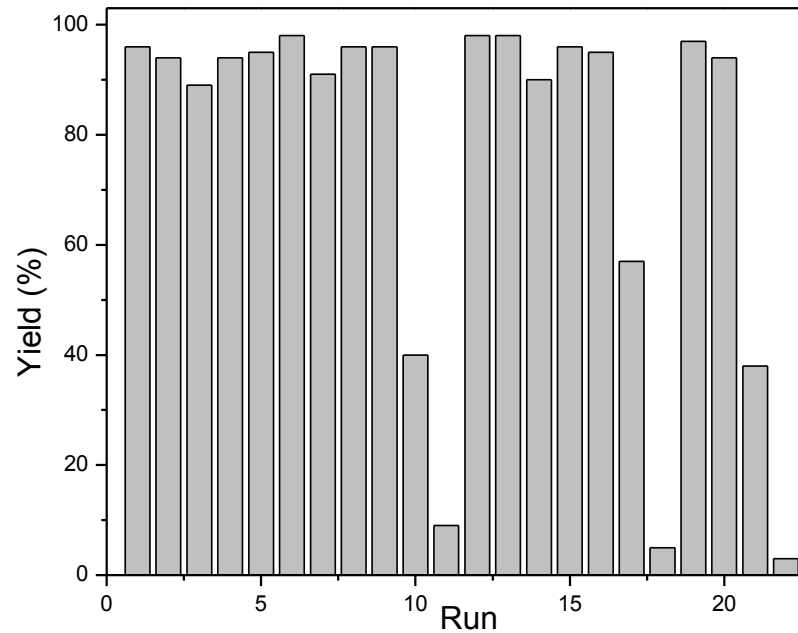
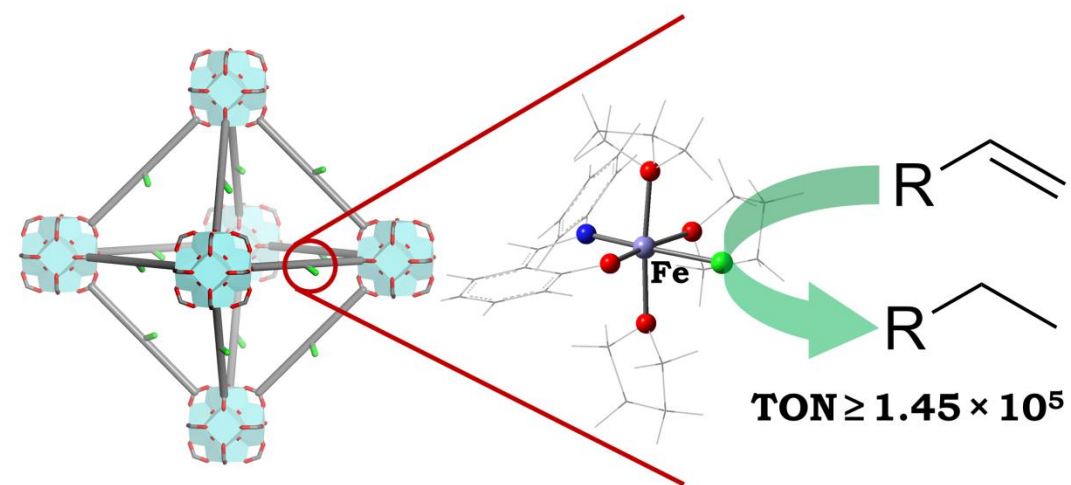


MOF-Enabled Olefin Hydrogenation with Fe and Co Catalysts

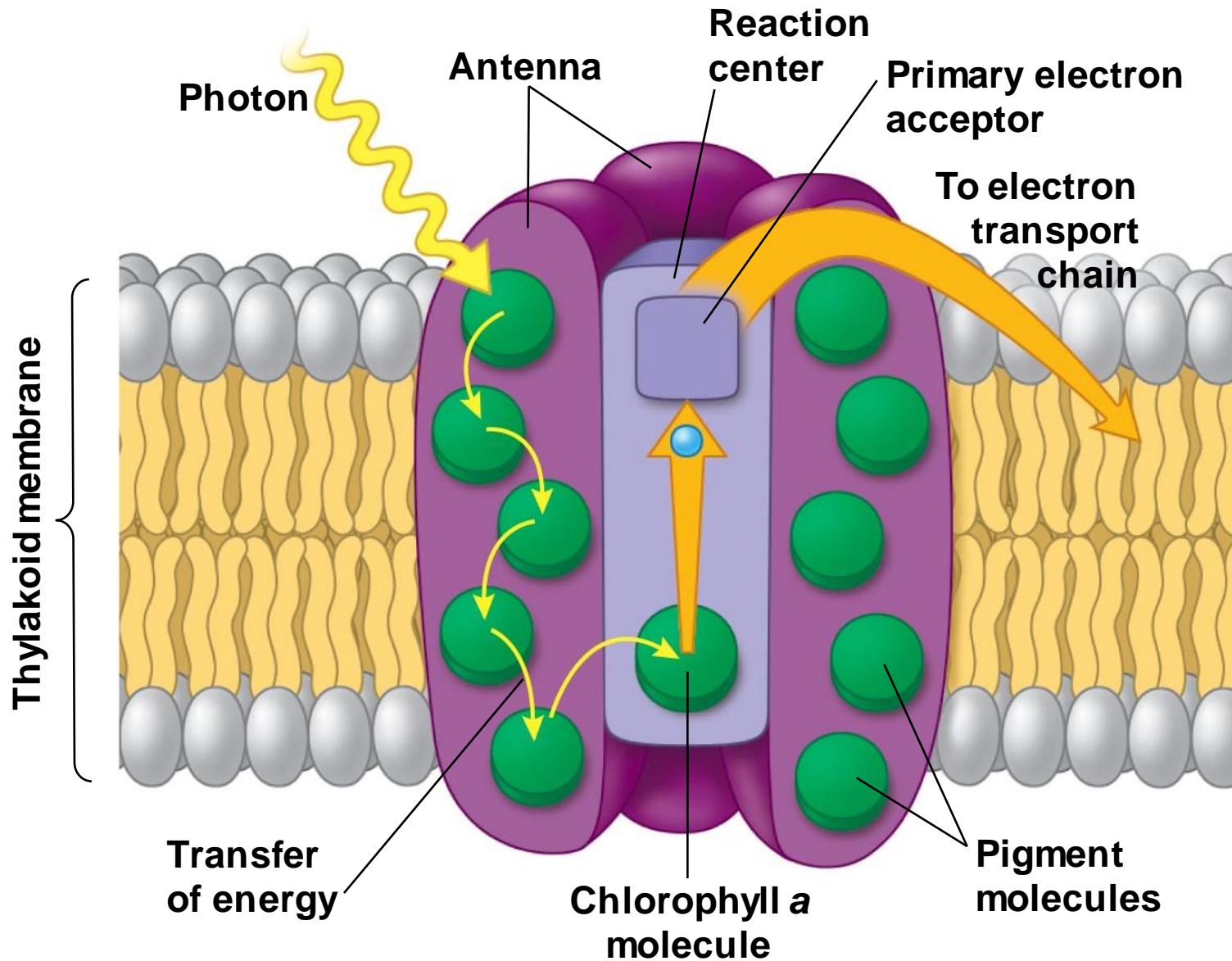


Entry	Substrate	M	Time	% Yield	TON
1		Fe	18 h	100	10000
2		Fe	8 d	94	145000 ^b
3		Co	18 h	75	25000
4		Fe	18 h	100	10000
5		Fe	24 h	44	44000 ^c
6		Co	18 h	55	18300
8		Fe	24 h	100	>10000
9		Co	18 h	100	>2000 ^e
10		Fe	18 h	100	>10000
11		Co	18 h	100	>2000 ^e
12		Fe	24 h	100	>2000 ^e
13		Co	18 h	100	>2000 ^e
14		Fe	24 h	100	>1000 ^f
15		Fe	18 h	100	>1000 ^f
16		Co	18 h	100	>2000 ^e
19		Fe	70 h	64	640 ^f
20		Co	72 h	0	0 ^e

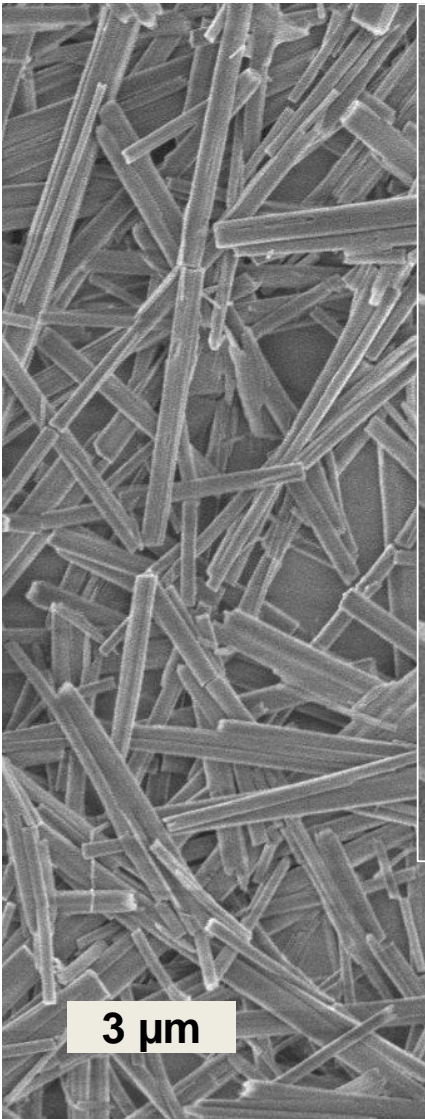
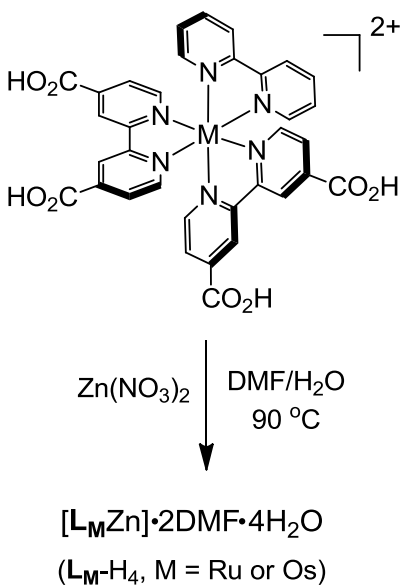
MOF-Enabled Olefin Hydrogenation with Fe and Co Catalysts



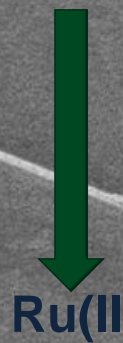
MOFs for Artificial Photosynthesis



Light Harvesting with Metal-Organic Frameworks

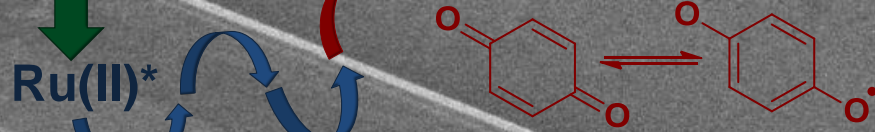


1. Photo-excitation

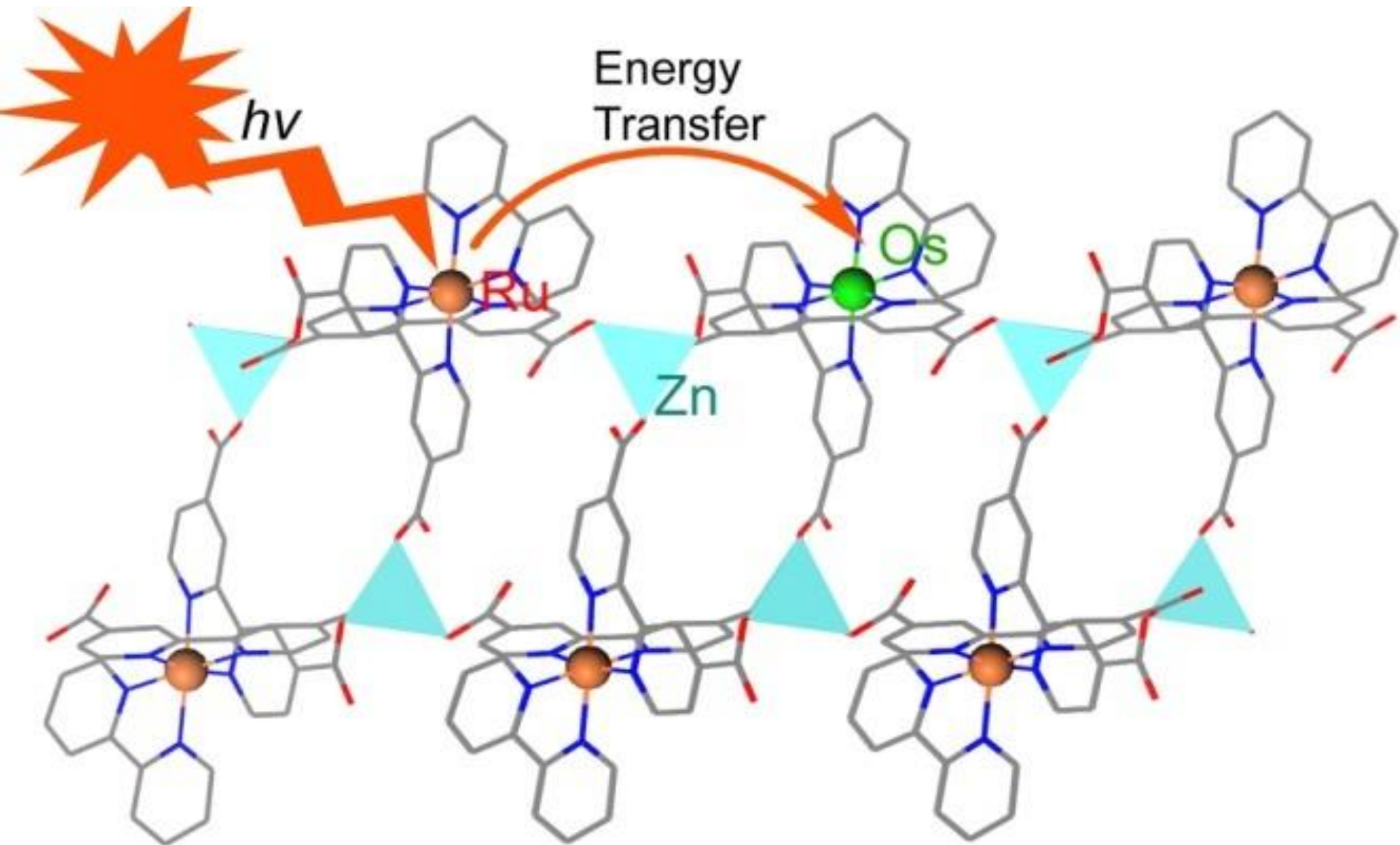


2. Excited state migration to Surface

3. Electron Transfer

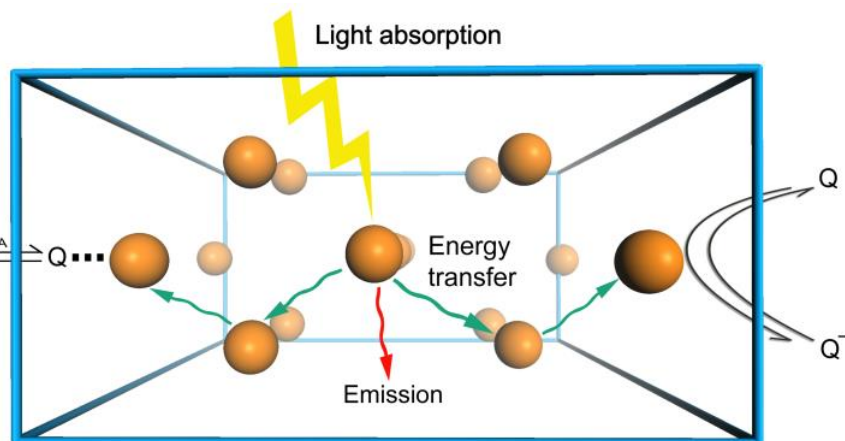


Rapid Energy Transfer in Phosphorescent MOFs

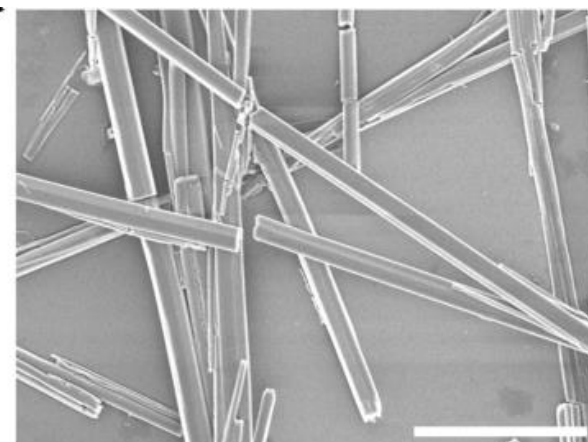
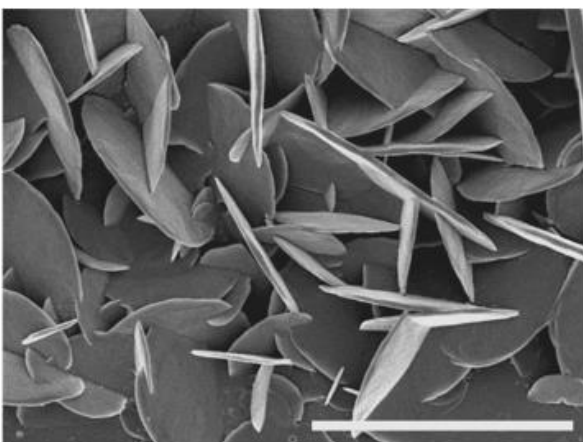
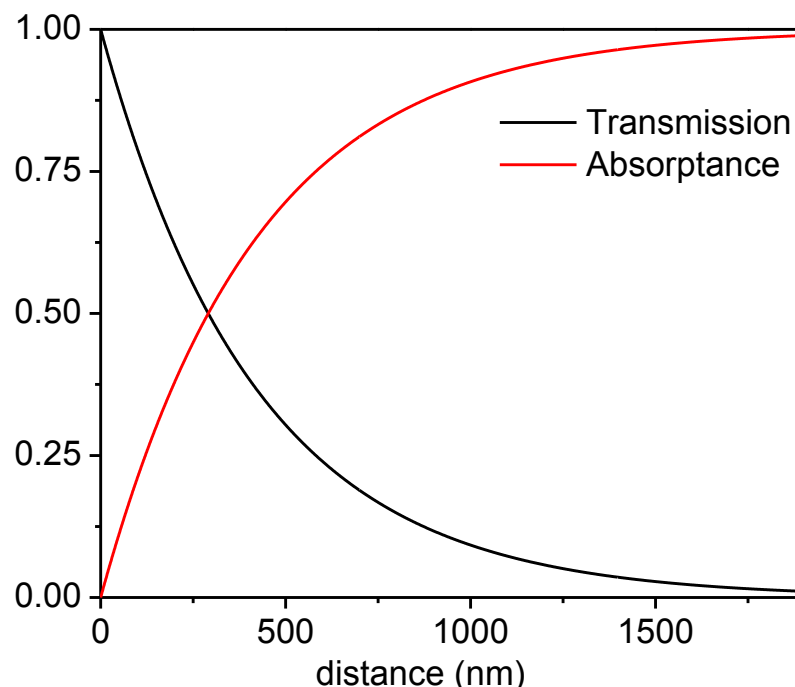
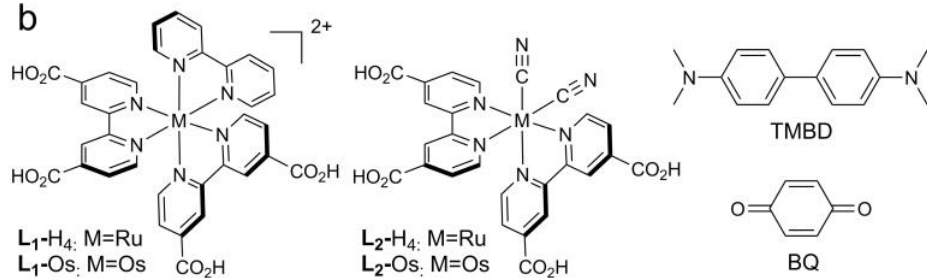


Light-Harvesting in Microscale MOFs by Energy Migration and Interfacial Electron Transfer Quenching

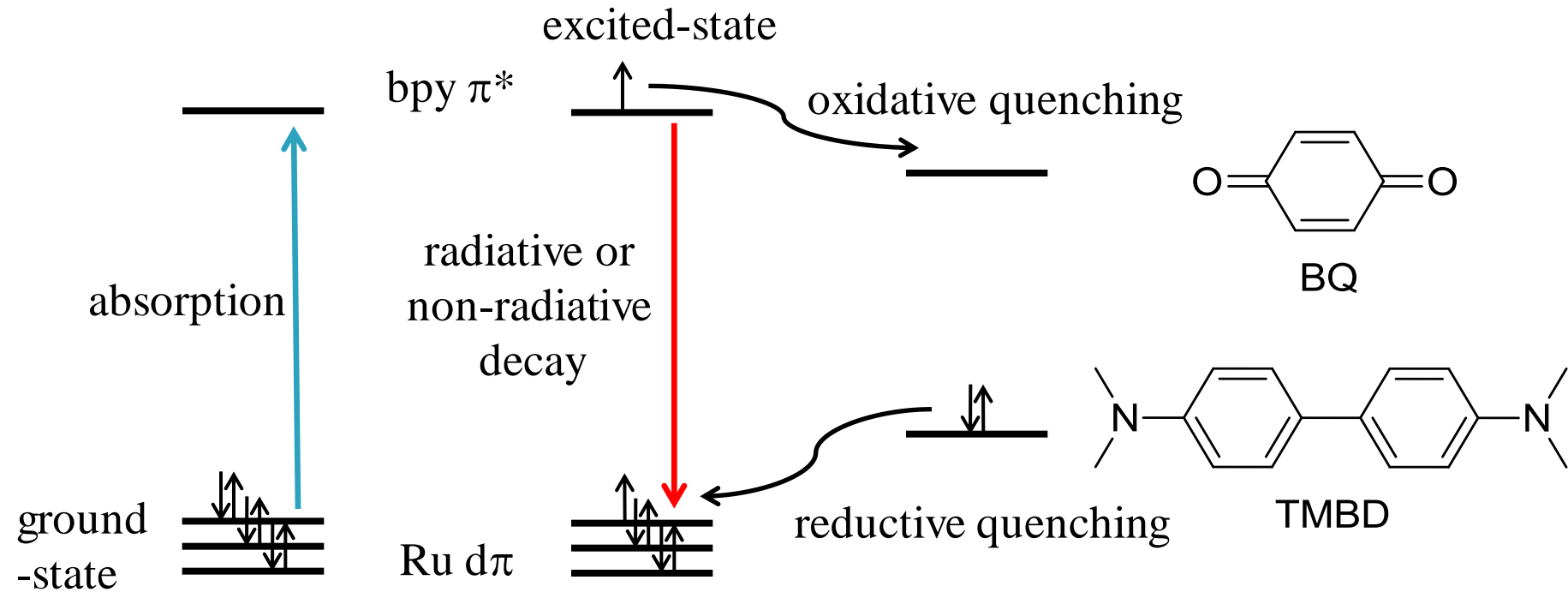
a



b



Excited-State Electron Transfer and Stern-Völmer Plots



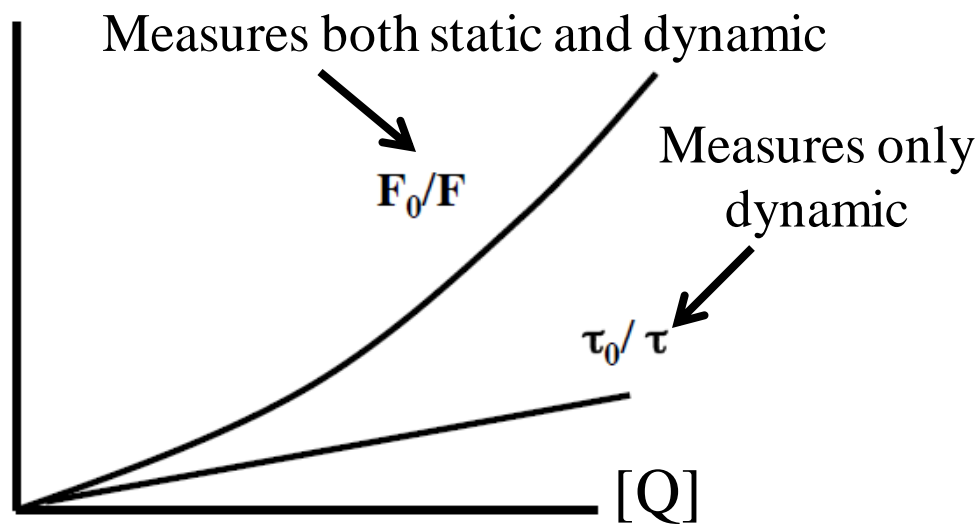
For purely dynamic quenching:

$$I_0/I = \tau_0/\tau$$

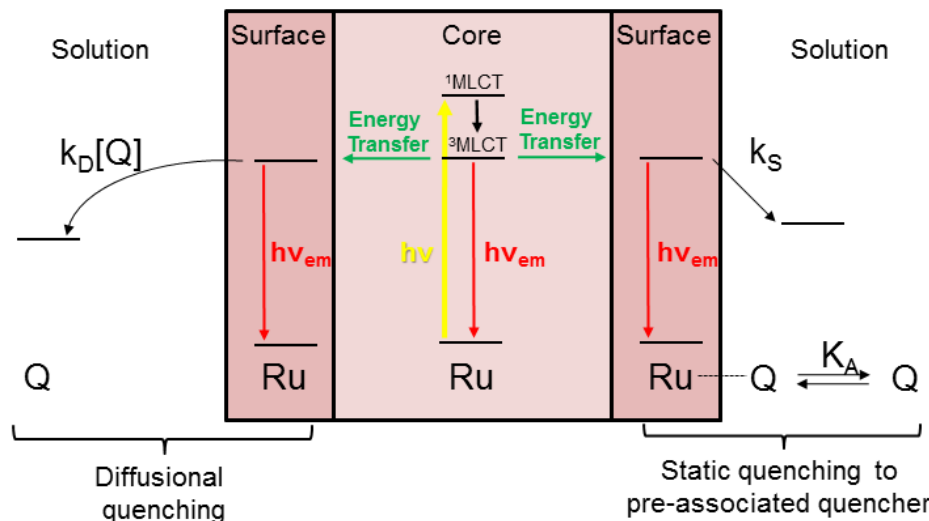
$$I_0/I = 1 + K_{sv}[Q] \quad K_{sv} = k_q \times \tau_0$$

For both static and dynamic:

$$I_0/I = (1 + K_{sv}[Q]) (1 + K_a[Q])$$



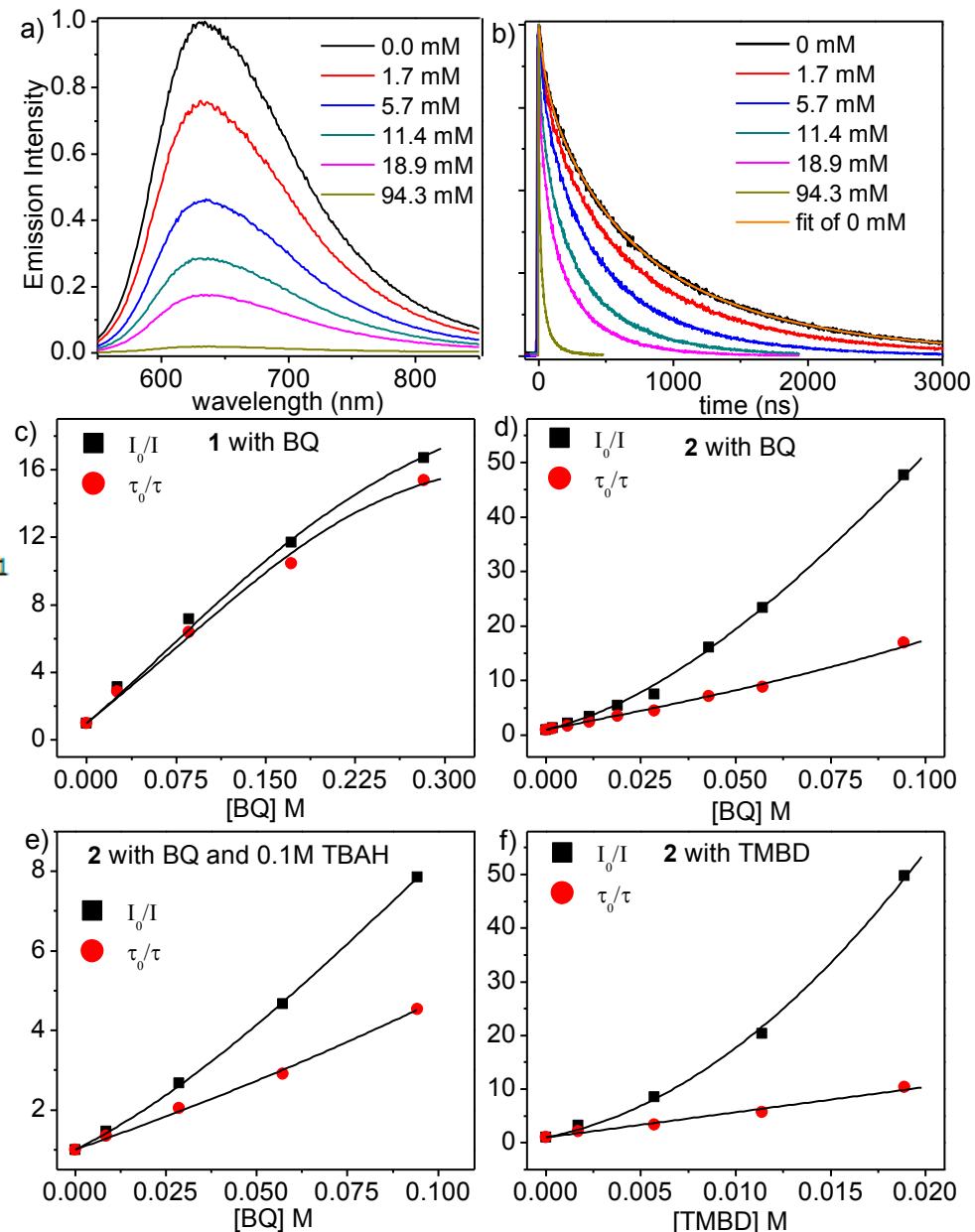
Light-Harvesting in Microscale MOFs by Energy Migration and Interfacial Electron Transfer Quenching



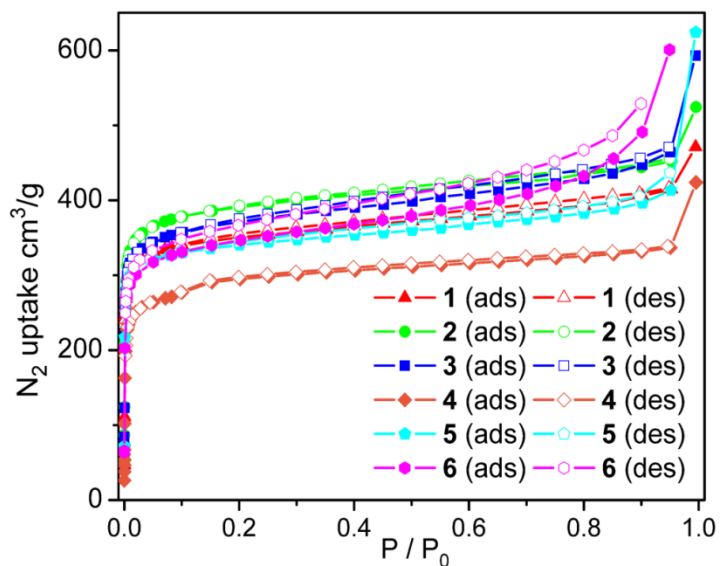
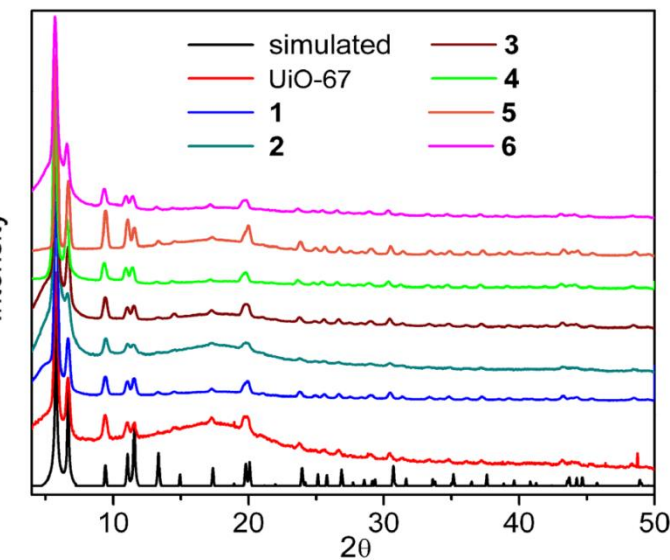
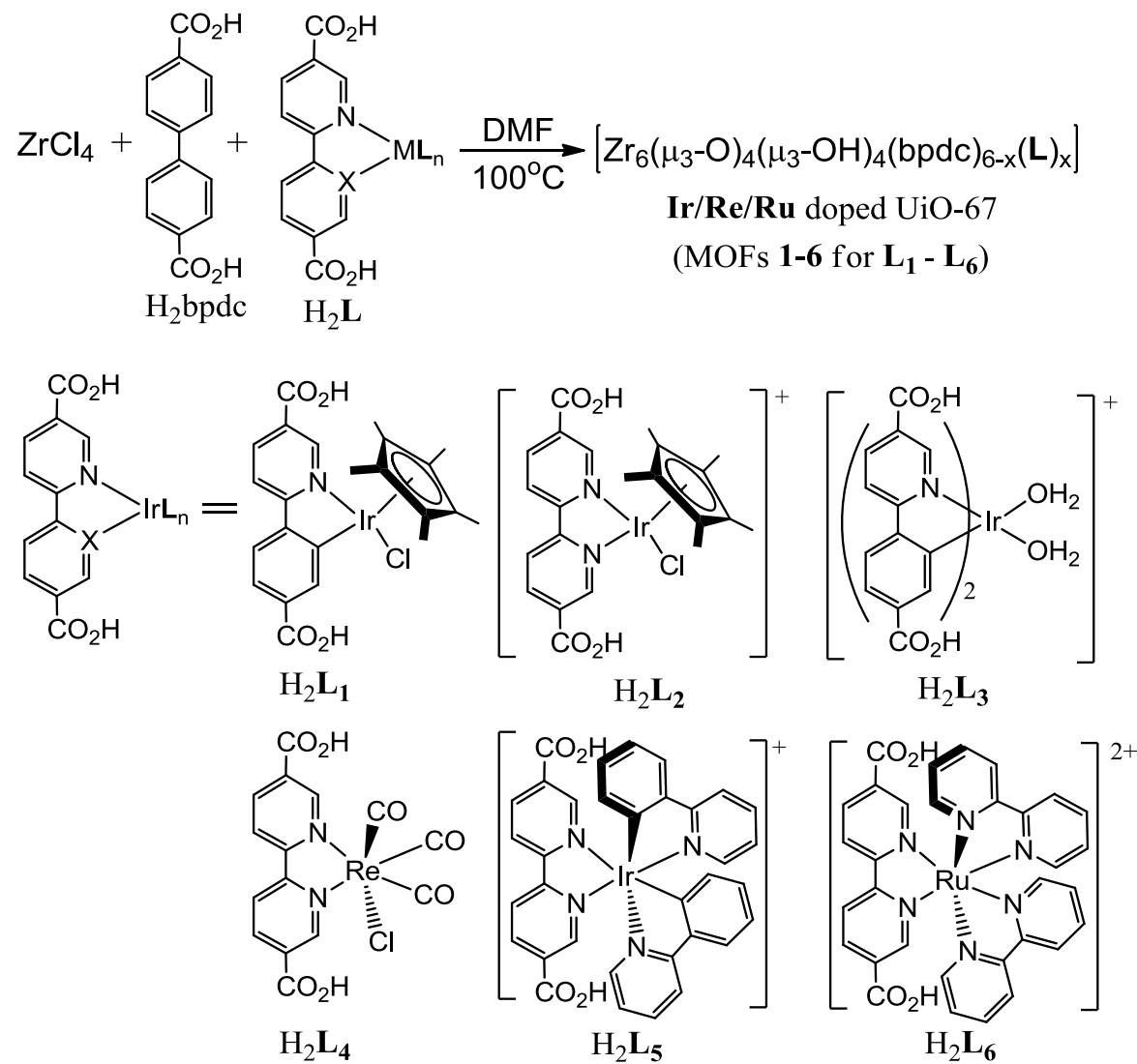
$$\frac{I_0}{I} = \left((1 - \gamma) + \gamma F_{SQ} \frac{k_{Ru^*}}{k_{Ru^*} + k_S} + \gamma (1 - F_{SQ}) \frac{k_{Ru^*}}{k_{Ru^*} + k_D[Q]} \right)^{-1}$$

$$\frac{\tau_0}{\tau} = \frac{1}{k_{Ru^*} \langle \tau \rangle}$$

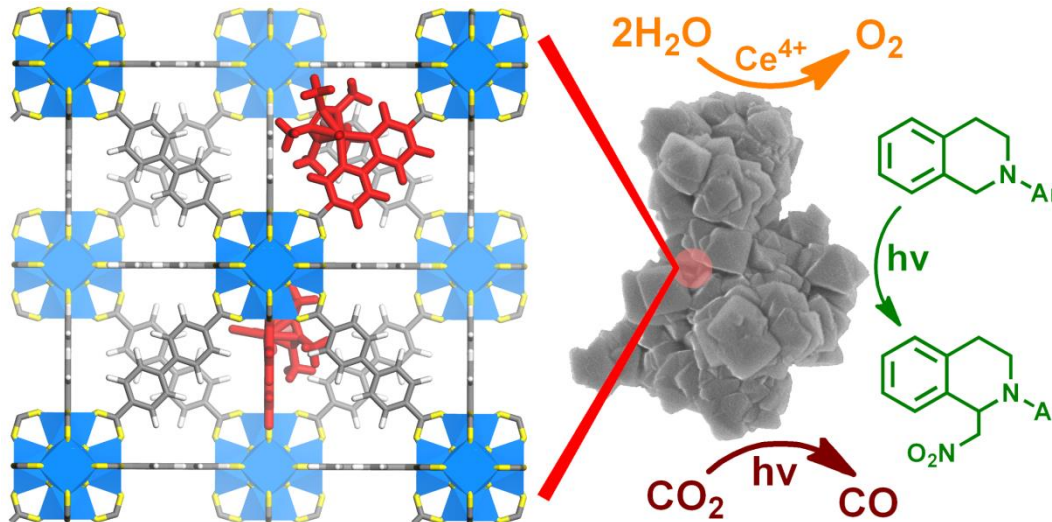
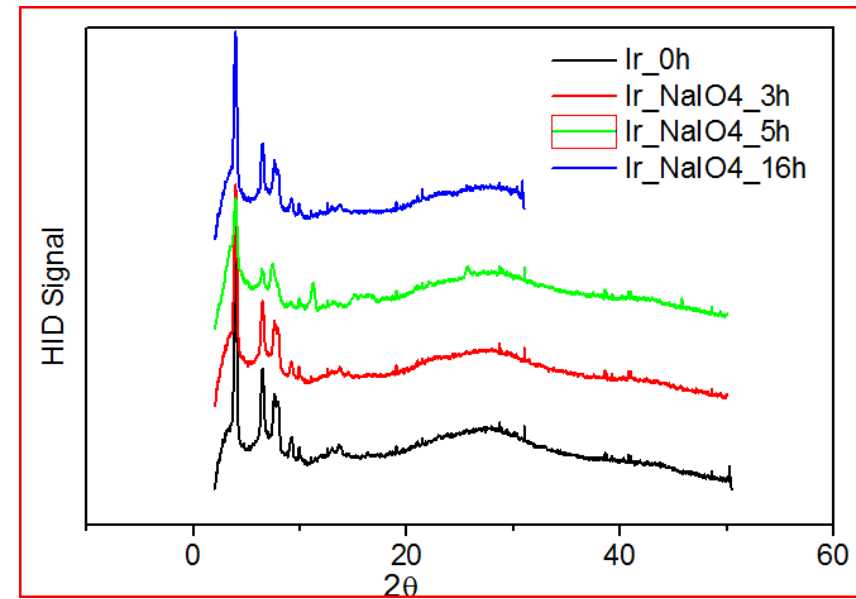
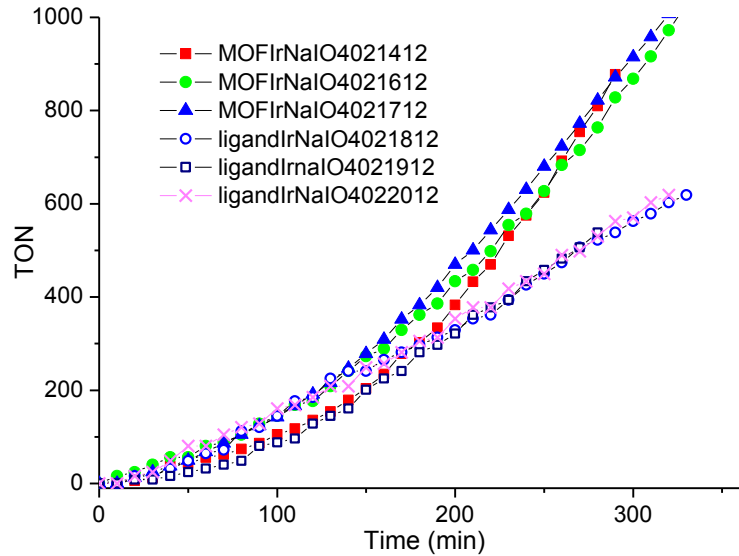
	K_A (M^{-1})	$1-\gamma$	k_S (ns^{-1})	k_D (10^7)
1 - BQ	1.9	1.00	0.0246	9.5
2 - BQ	32.4	1.00	0.2080	12.4
2 BQ/T	13.7	1.00	0.0265	2.9
2 - TM	211	1.00	>15	42.6



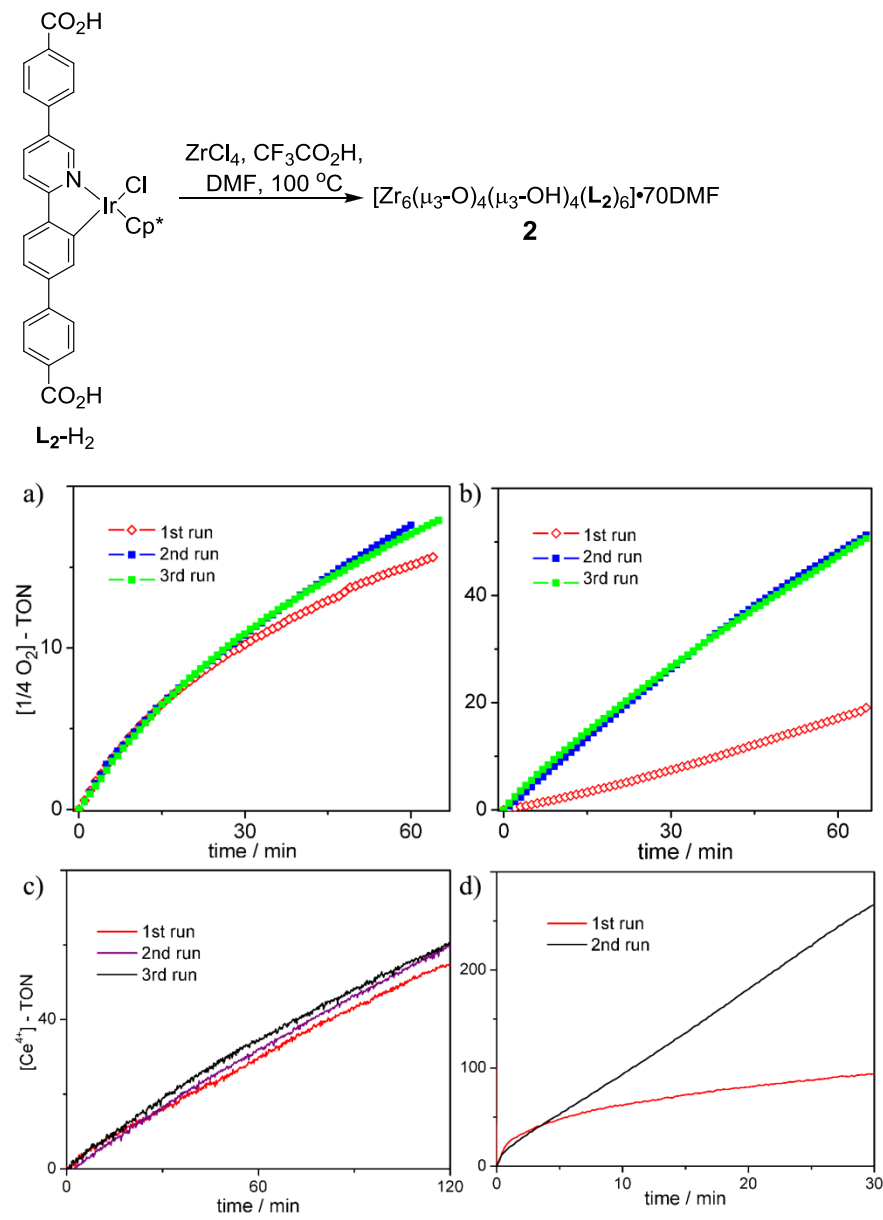
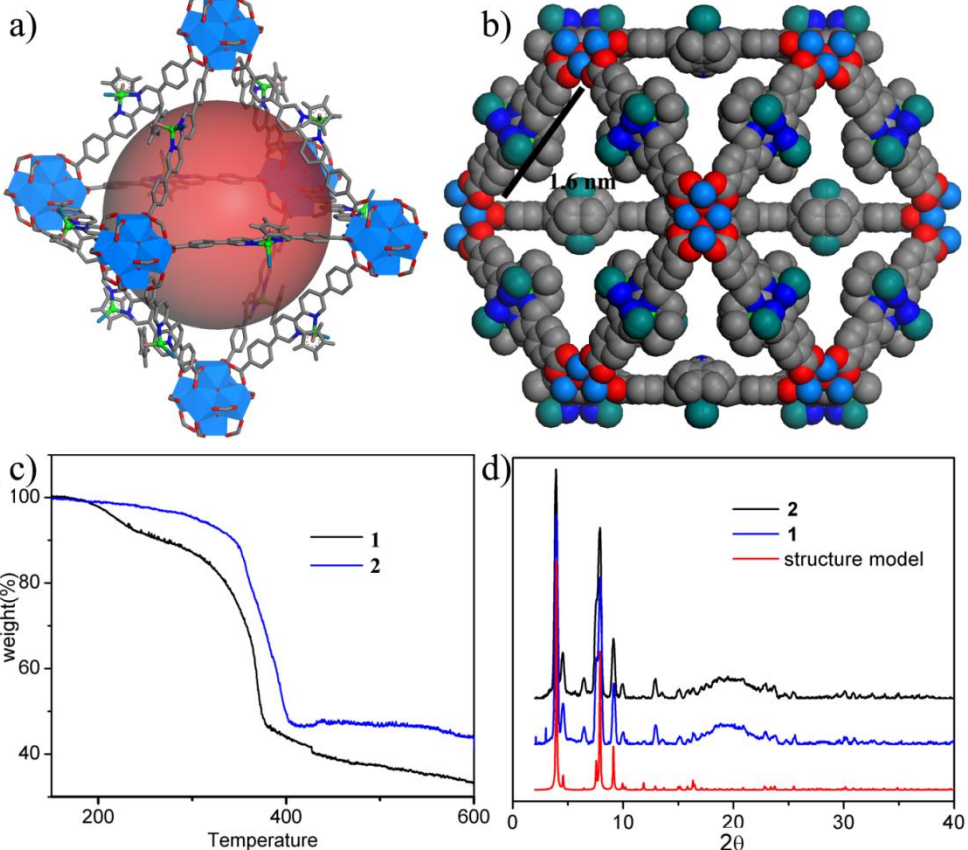
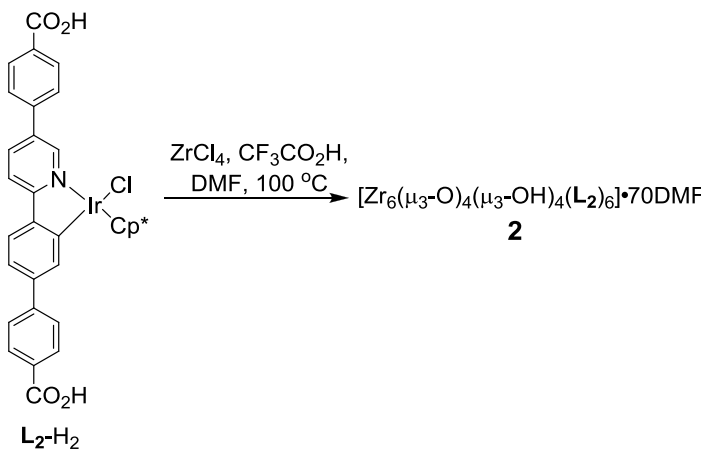
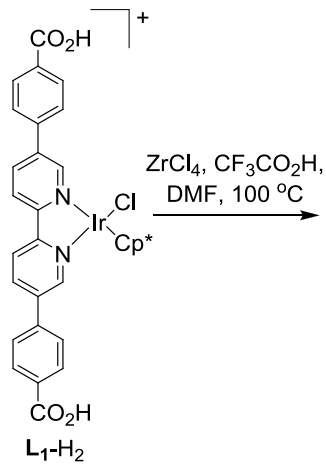
MOFs for Water Oxidation and Photocatalysis



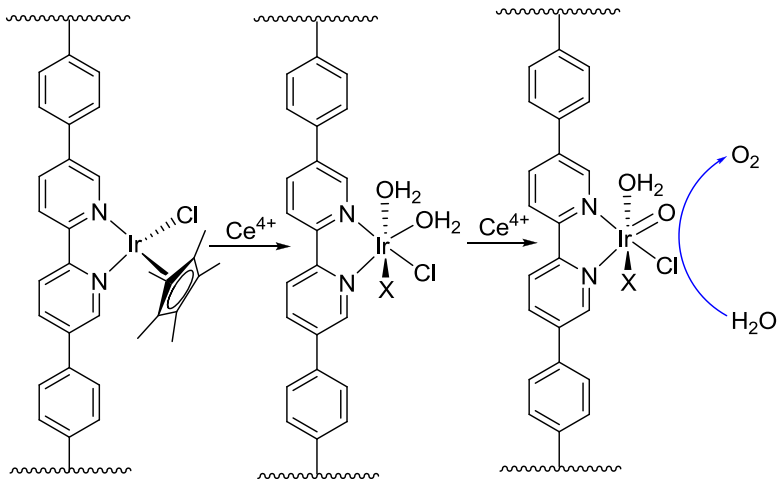
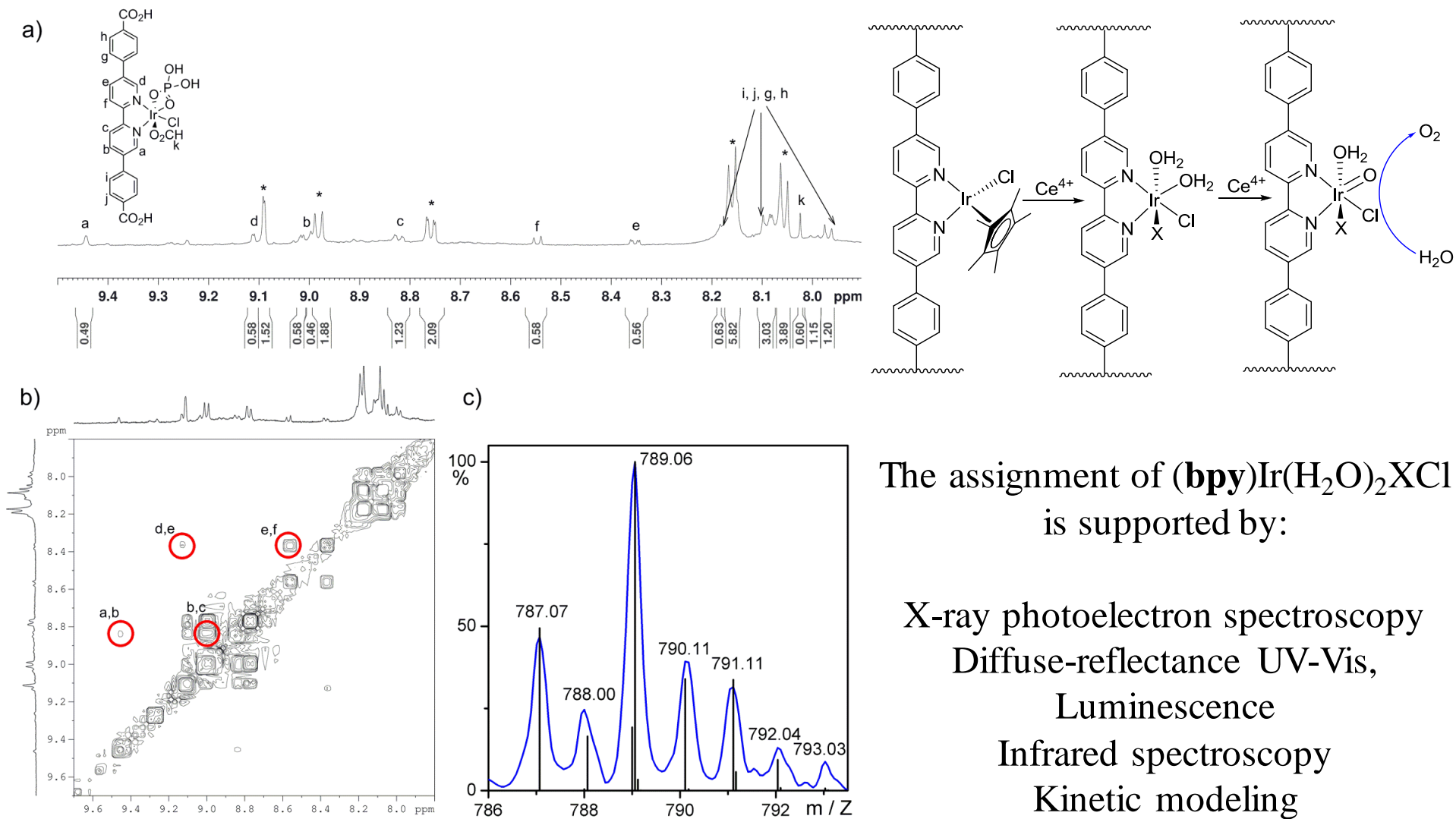
MOFs for Water Oxidation and CO₂ Reduction



Elucidating Molecular Iridium Water Oxidation Catalysts Using MOFs



Identification of $(bpy)Ir(H_2O)_2XCl$ as an active water oxidation catalyst



The assignment of $(bpy)Ir(H_2O)_2XCl$ is supported by:

X-ray photoelectron spectroscopy
Diffuse-reflectance UV-Vis,
Luminescence
Infrared spectroscopy
Kinetic modeling

A Diffusion-Reaction Kinetic Model Explains Partial WOC Modifications

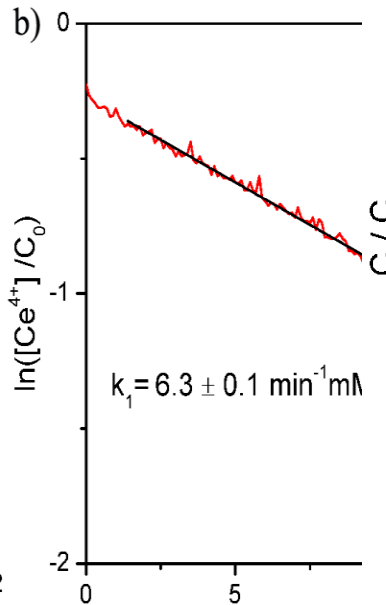
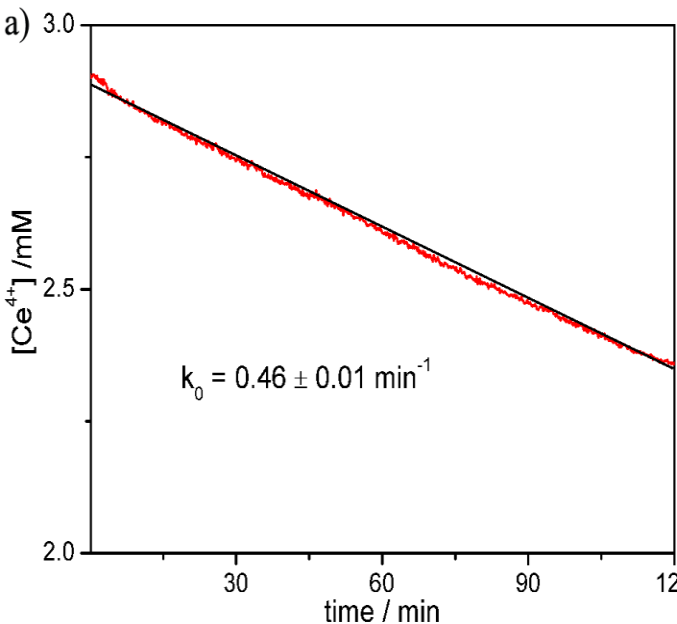
$$\frac{\partial c(r,t)}{\partial t} = D \frac{1}{r^2} \frac{\partial}{\partial r} \left(r^2 \frac{\partial c(r,t)}{\partial r} \right) - kc(r,t)$$

$$t = 0 \quad 0 < r < a, \quad c = 0; \quad r = a, \quad c = c_0$$

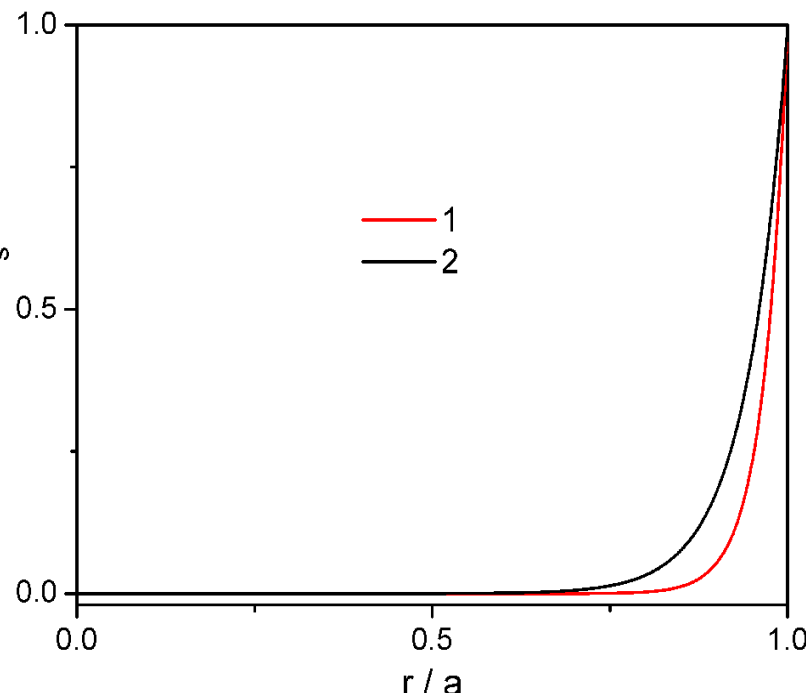
$$r = a, \quad V \frac{\partial c(r,t)}{\partial t} = -N \cdot 4\pi a^2 D \frac{\partial c(r,t)}{\partial r}$$

For 1: $\frac{d\frac{c_s}{c_0}}{dt} = -\beta \frac{\sqrt{kD}}{a} \left(1 - \frac{1}{a} \sqrt{\frac{D}{k}}\right)$

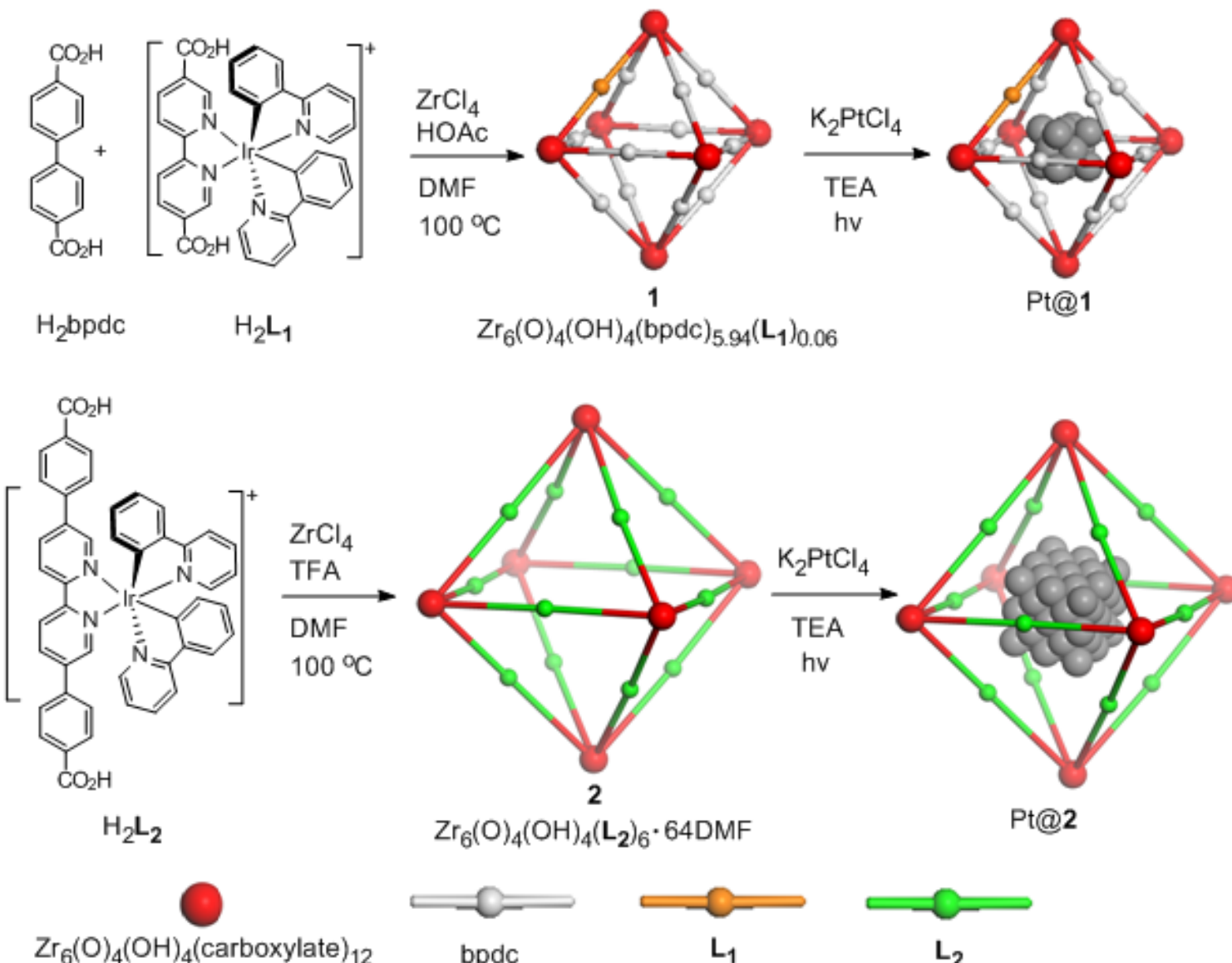
For 2: $\frac{d\ln\left(\frac{c_s}{c_0}\right)}{dt} = -\beta \frac{\sqrt{kD}}{a} \left(1 - \frac{1}{a} \sqrt{\frac{D}{k}}\right)$



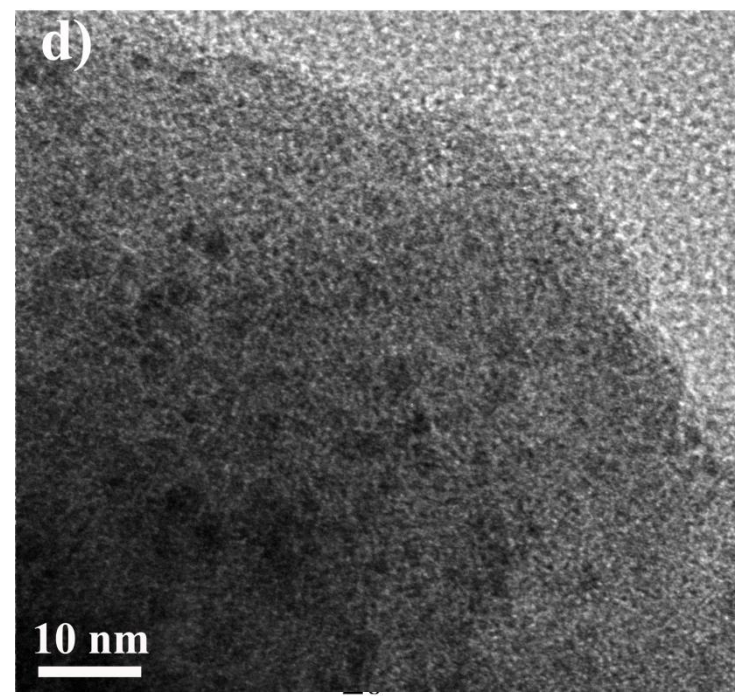
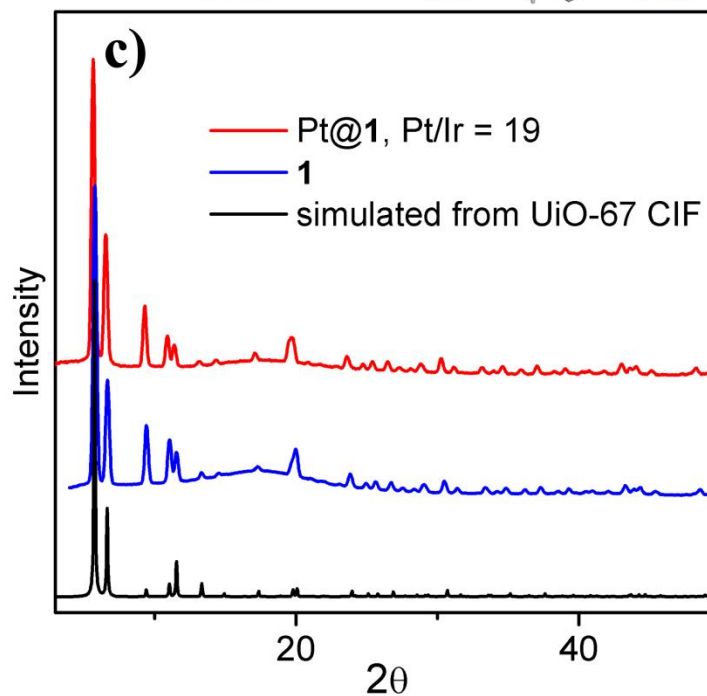
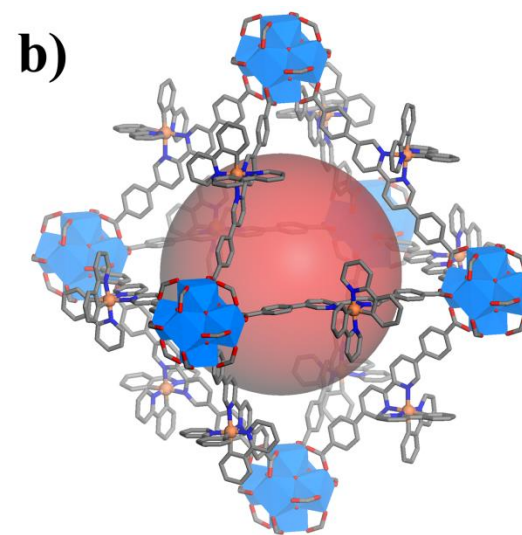
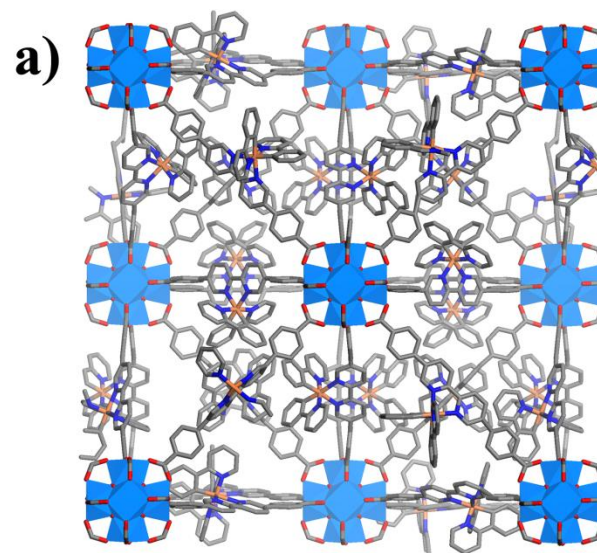
1		2	
c_0 (mM)	D (/10 ⁻¹¹ cm ² s ⁻¹)	c_0 (mM)	D (/10 ⁻¹¹ cm ² s ⁻¹)
0.29	1.52	0.11	67.9
0.98	0.221	0.30	38.8
2.03	0.099	0.40	41.0
2.88	0.053	0.51	4.6
4.61	0.050	0.61	4.1
5.69	0.046	1.09	3.4
6.97	0.046		



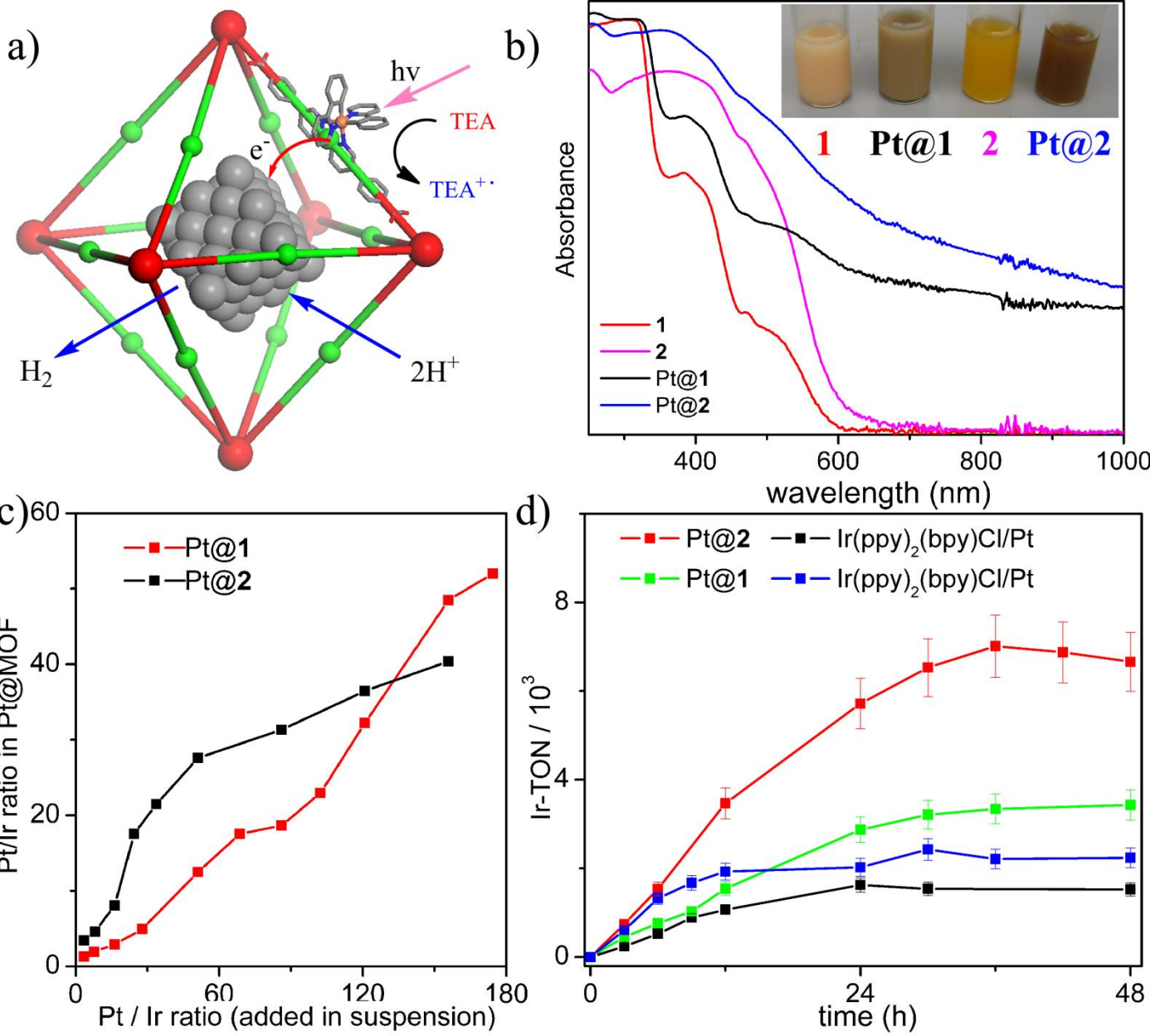
Synthesis of Pt Nanoparticle@Photoactive MOFs



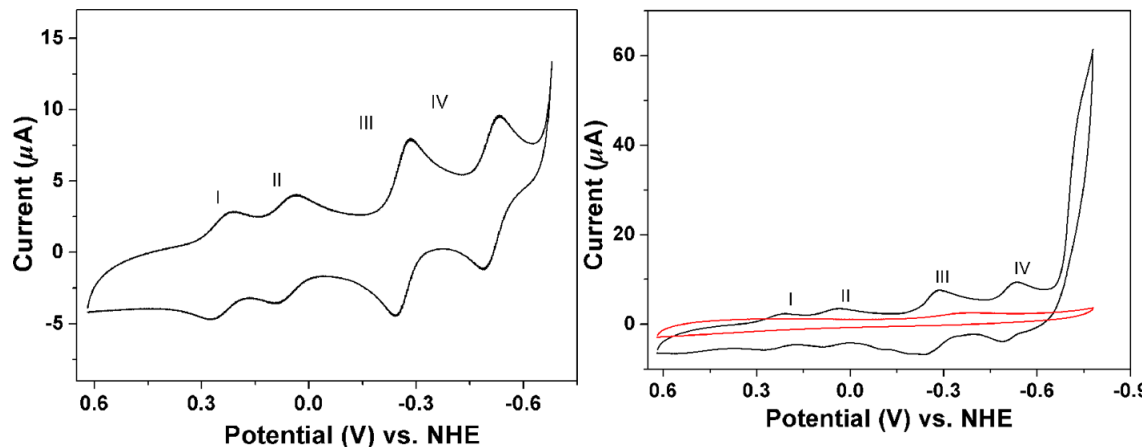
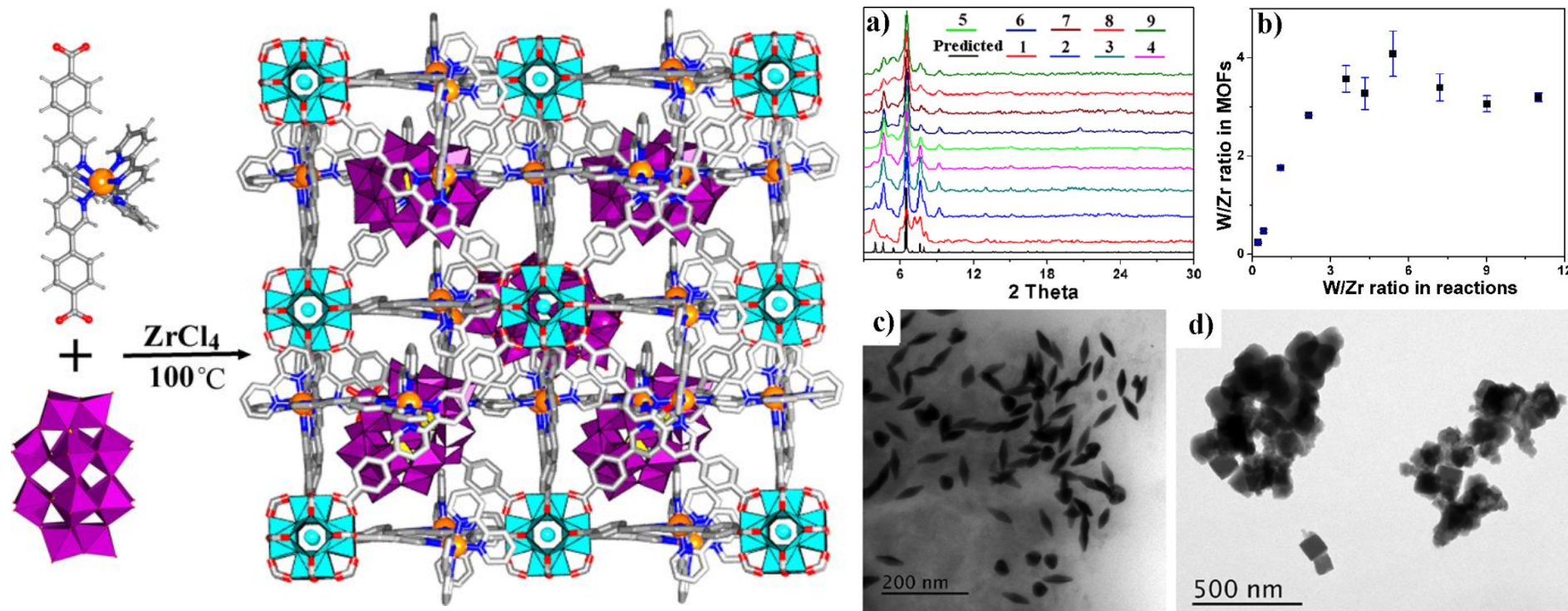
Characterization of Pt Nanoparticle@Photoactive MOFs



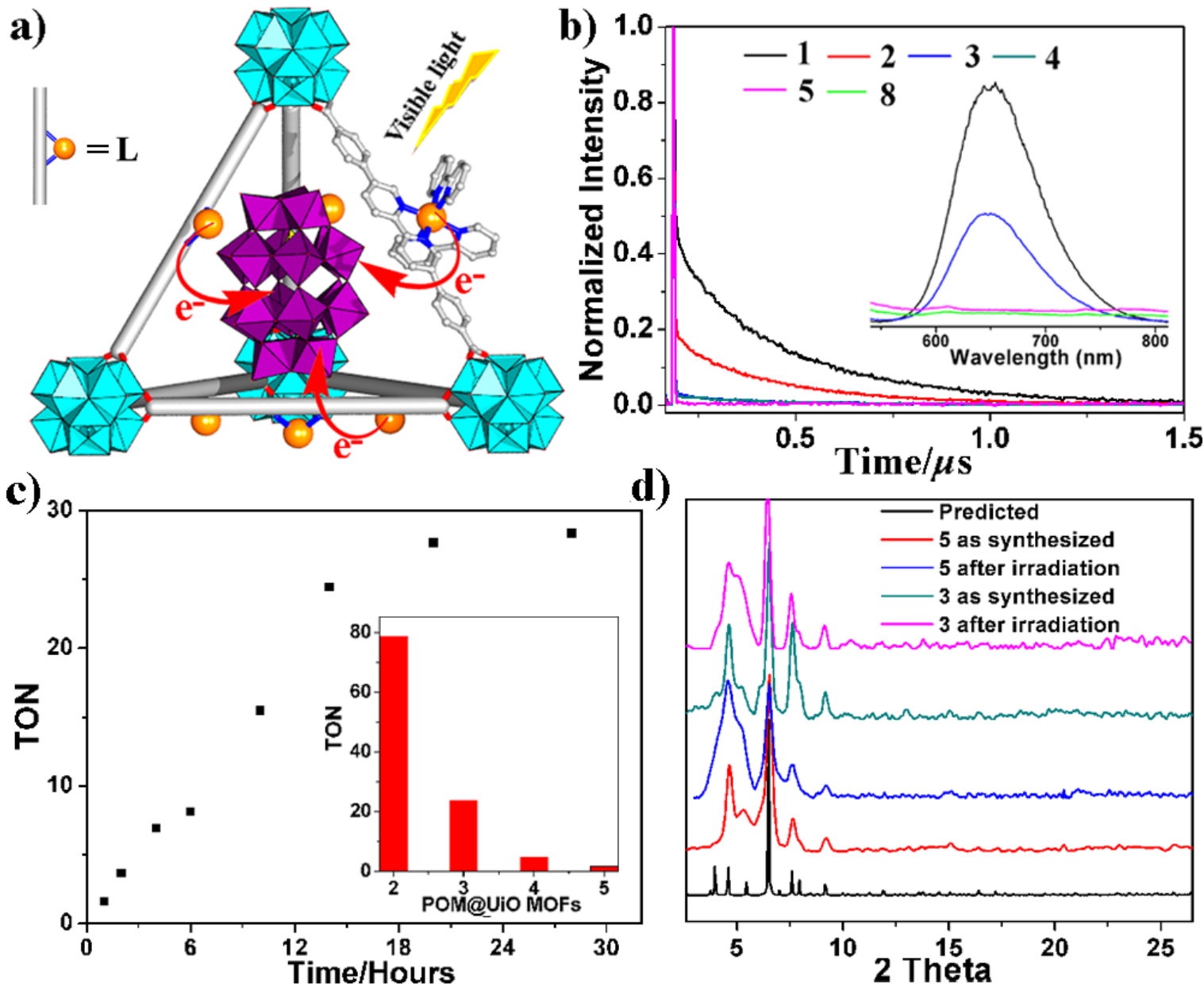
Efficient Hydrogen Evolution via Synergistic Photo-excitation and Electron Injection



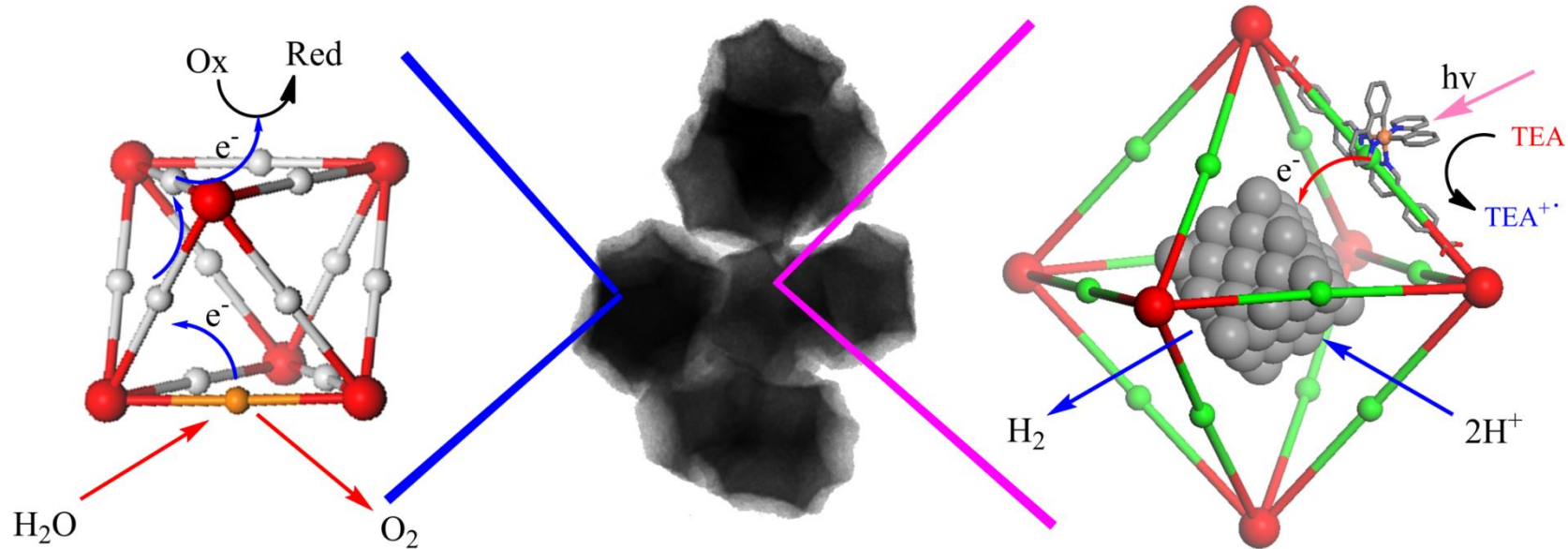
Photosensitizing MOF Enabling Visible-Light Driven Proton Reduction by A Wells-Dawson-Type Polyoxometalate



Photosensitizing MOF Enabling Visible-Light Driven Proton Reduction by A Wells-Dawson-Type Polyoxometalate



Combining Light-harvesting Antenna and Reactive Centers for Water Splitting and CO₂ Reduction?



- ◆ Photosensitizing MOFs with built-in water oxidation catalysts and encapsulated proton reduction (e.g., Pt) catalysts for water splitting.
- ◆ Integration of these components into the same framework and the DSPEC platform for total water splitting and CO₂ reduction.

Acknowledgements

Dr. Takahiro Sawano

Dr. Kuntal Manna

Dr. Nathan Thacker

Pengfei Ji

Frank Greene (UG)

Teng Zhang

Zekai Lin

Daniel Micheroni

Xin Zhao

Dr. Xiangjian Kong

Marek Piechowicz

Carter Abney

Connor Gilhula (UG)

Kuangda Lu

Chris Poon

Dr. Chunbai He

Dr. Jianqin Lu

Christina Chan

Ruoyu Xu

Alexander Chen (UG)

Christine Ma (UG)



NSF-CHE: MOFs for asymmetric catalysis

NSF-DMR: Framework materials for solar fuels

NSF-DMR: Fundamental studies of Nano-MOFs

NCI-U01: Nano-MOFs for pancreatic cancer

DOE-NE: Porous sorbents for uranium extraction

USDA: Sustainable Synthesis of Biolubricants